This article has been accepted for publication in IEEE Transactions on Wireless Communications. This is the author's version which has not been fully edited and content may change prior to final publication. Citation information: DOI 10.1109/TWC.2023.3250659

Concatenative Complete Complementary Code Division Multiple Access and its Fast Transform

Hikaru Mizuyoshi and Chenggao Han

***Abstract*—Over multipath channels, complete complementary code division multiple access and convolutional spreading code division multiple access provide inter-channel interference free transmission with an enhanced spectral efficiency. However, the *convolutional spreading* (CS) operation of the systems is computationally complex and involves a high peak-to-average power ratio. To address such issues, we propose the *concatenative complete complementary code* (CCCC) division multiple access, named (CCC-CDMA). Since the CCCCs can be generated from the rows of the Walsh-Hadamard or discrete Fourier transform matrices, the CS operation can be implemented using corresponding fast transforms to reduce computational complexity. Simulation results show that the enlargement of the spreading factor strengthens the robustness against clipping noise. The binary CCCC generated by Walsh-Hadamard matrix exhibited excellent robustness against Doppler frequency shifts.**

***Index Terms*—CDMA, complete complementary codes, zero correlation zone sequences, CC-CDMA, CS-CDMA**

I. INTRODUCTION

A. Background

Code division multiple access (CDMA) and *orthogonal frequency division multiple access* (OFDMA) are two major multiplexing schemes of current digital communication system. When comparing *direct spread* (DS)-CDMA with OFDMA, DS-CDMA distinguishes users based on the previously assigned signals, called *spreading sequences*, while the indexes of frequency sub-carrier are used for user identification in OFDMA. More specifically, CDMA multiplies each user's modulated symbols by the corresponding spreading sequence while those are multiplied by several one-to-one sinusoidal waves. Thus, if we treat the sampled sinusoidal waves/signals as spreading sequences in a unified manner, the essential differences between DS-CDMA and OFDMA are as follows:

1) Number of spreading sequences
   Since each user transmits modulated symbols over multiple sub-carriers, OFDMA assigns multiple sequences while a single sequence is assigned to each user in DS-CDMA.
2) Synchronization
   Each OFDMA packet is composed of synchronously summarized spread signals, and the transmitted symbols are detected synchronously at the receiver. Meanwhile, DS-CDMA transmits the spread signals asynchronously. Hence, synchronization is not required at both sides.
3) The *cyclic prefix* (CP) scheme
   An OFDM-based system utilizes the CP scheme to convert the aperiodic convolution between the transmitted packet and *channel impulse response* (CIR) into periodic convolution.

H. Mizuyoshi and C. Han was with the Graduate School of Informatics and Engineering, The University of Electro-Communications, 1-5-1 Chofugaoka, Chofu-shi, Tokyo, 182–8585, Japan, Email: {mizuyoshi, han.ic}@uec.ac.jp

Therefore, we may regard OFDMA as a special CDMA that assigns multiple sinusoidal signals for each user, transmits and receives signals in the synchronous manner, and employs CP scheme.

In terms of signal design, the performance of CDMA over multipath channel primarily depends on the correlation properties of the employed spreading sequences. The maximum *spectral efficiency* (SE) [1] can be achieved by a *sequence set* (SS) with the ideal correlation properties. In other words, the auto-correlation function of each sequence is zero except at zero shift, and the cross-correlation functions of any distinct sequence pair are zero at all shifts. Unfortunately, such an SS is non-existent, and instead, the pseudo-random sequences which have small side-lobes, *e.g.*, Gold sequences, Kasami sequences, and *maximum-length sequences* (M-sequences) [2], were widely employed for DS-CDMA.

Even the side-lobes of the pseudo-random sequence are designed as a small value, the non-ideal cross-correlation causes *inter-channel interference* (ICI) and involves a near-far problem. Thus, DS-CDMA can be classified as an ICI limited system since the overall cell capacity cannot be increased by increasing the transmission powers. Therefore, a complex power control unit is essential to combat the near-far problem. On the contrary, OFDMA utilizes the sinusoidal waves that have the ideal periodic cross-correlation property and is an ICI-free system.

While the cross-correlation property of the employed spreading sequences is associated with ICI, the auto-correlation property affects the accuracy of detected symbols over multipath channels. Accordingly, DS-CDMA spreads the modulated symbols using the sequences that have sharp auto-correlation and it generally attains full path diversity over a multipath fading channel, *i.e.*, the order is equal to the number of independent paths. Meanwhile, since the periodic auto-correlations of the sinusoidal waves are constant in amplitude across all shifts the achievable diversity order of the naive OFDM/OFDMA is only one. Therefore, in the practical uses of OFDM/OFDMA, codings over sub-carriers is usually applied to improve the attainable diversity order [3], [4]. Nevertheless, obtaining the full path diversity for OFDM/OFDMA is not a easy task [5], [6].

B. Related works

The signals with the ideal correlation properties have been investigated by numerous researchers to realize ICI-free communication systems. Such approaches can be classified into two classes: *complete complementary code* (CCC) [7]–[10] and *zero-correlation zone* (ZCZ) sequences [11]–[13]. The former utilizes multiple sequences to realize an *ideal correlation sum* while the ideal correlation properties are designed to achieve on ZCZ in periodic manner for the latter.

The CCC-based ICI-free system, called *complete complementary coded CDMA* (CC-CDMA), was proposed by Suehiro *et al.* in [14], [15]. In CC-CDMA, each sub-packet spread by a different sequence should be passed through an individual matched filter. Since as the separation of sub-packets is completed on time or frequency domain, it can be further classified into two categories: *time division multiplex* CC-CDMA [15] and *frequency division multiplex* CC-CDMA [16]. The former requires *zero padding* (ZP) or CP schemes for each sub-packet to prevent inter-sub-packet interferences cause by multipath propagation, and hence, it is inferior to latter in terms of SE but is superior in system performance and implementation complexity [17]–[19].

The concept of ZCZ sequences first appeared in [11] and originally applied to realize ICI-free *quasi-synchronous* CDMA to maintain the orthogonality between channels if user's time delays occur within a few chips [20], [21]. Subsequently, the ZCZ sequence based CDMA with *convolutional spreading* (CS) scheme [15] was investigated by Weerashinghe *et al.* termed as CS-CDMA [22], [23]. The authors show that associate with multiple-input single-output, CS-CDMA provides complete transmit and path diversities [24]. Later, Yue *et al.* realized an SE higher than DS-CDMA and *chip-interleaved block spread* CDMA proposed in [25] by utilizing *iterative partial multiuser detection* to CS-CDMA [26].

Both CC- and CS-CDMAs utilize the CS scheme to achieve a high SE, which involves high *peak-to-average power ratio* (PAPR). Accordingly, Weerasinghe *et al.* investigated the robustness against clipping noise for various ZCZ sequences and indicated that the *M-sequence based ZCZ* (M-ZCZ) sequence as the most robust [27]. Moreover, the sequence selection also affects the performance of CS-CDMA over fast fading channels and the inferior-to-superior association is related to the use of a channel estimation at the receiver. Without channel estimation, M-ZCZ is superior to the ZCZ sequences constructed from a Chu sequence [28], as noted by Chu-ZCZ, while an elaborately designed channel estimation reverses the superiority [29]–[31].

A key difference between CC- and CS-CDMA is that, in CC-CDMA, each user utilizes multiple spreading sequences as well as OFDMA while a single sequence is used in CS-CDMA. Consequently, CC-CDMA requires multiple CPs/ZPs to prevent inter-sub-packet interferences over multipach channels while single CP is required for each packet in CS-CDMA, and generally, CS-CDMA achieves higher SE than CC-CDMA. Moreover, since a larger ZCZ of the employed SS translates to a higher SE of CS-CDMA, we desire a simple construction of ZCZ sequences with the largest ZCZ.

On the other hand, Han *et al.* have proposed a special class of CCC, named *concatenative CCC* (CCCC), and constructed the binary and polyphase CCCCs using *Walsh Hadamard* (WH) and *discrete Fourier transform* (DFT) matrices, respectively [32]. In given CCCC, ZCZ sequences can be constructed by concatenating the sequences in each complementary code set and elongating ZCZ by padding zeros for each sequence before concatenation. Thus, in association with the CS-CDMA scheme, the *concatenative complete complementary code division multiple access* (CCC-CDMA) provides a simple ZP scheme to enhance SE. Furthermore, Han *et al.* proposed an OFDM like *fast Fourier transform* based implementation structure for the transmitter of CCC-CDMA to reduce the computational complexity of the CS operation, and showed a trade-off relationship between clipping resistance and computational complexity [33], [34].

C. Contributions

In this study, we present a comprehensive *fast transform* (FT) based transceiver structures of both binary and polyphase CCC-CDMAs by introducing interleaver/deinterleaver components. We prove that the outputs of the proposed structure are equivalent to that of the CS-CDMA employing the ZCZ sequences constructed from CCCC and provide the performance and complexity analysis under assumption that the *maximum likelihood* (ML) detection is employed at the receiver. The numerical results indicate that CCC-CDMA enhances the resistance against clipping noise by simply incrementing of the employed sequence length *i.e.*, increment of *spreading factor* (SF), and the binary CCC-CDMA has excellent robustness against Doppler frequency shifts. Compared with OFDMA, the proposed CCC-CDMA is also a synchronous multiple access transmission that can be implemented by FTs, however, it is superior to OFDMA at the achievable diversity order over multipath fading channel, and serves as a simple countermeasure against clipping noise while being robust against frequency shifts.

D. Paper Organization

The remainder of this paper is organized as follows. In Section II, after defining the correlation and correlation sum, we introduce some sequence set/family with ideal correlation (sum). In Section III, we briefly review the conventional CC-CDMA and CS-CDMA. In Section IV, we present the novel FT-based tranceiver structures of CCC-CDMA. The performance of CCC-CDMA over Reighy fading multipath channel is analyzed in Section V. The numerical results are shown in Section VI and, finally, we conclude this study in Section VII.

E. Notations

A vector is denoted by a bold lowercase letter and is also represented with its entries as $\boldsymbol{v} = (v_n)_{n=0}^{N-1}$. $\mathbf{0}_N$ denotes an all zero vector of length N. For given vector $\boldsymbol{v}$, let $\boldsymbol{v}(a:b) = (v_n)_{n=a}^{b}$ be the length-$(b-a+1)$ partial vector of $\boldsymbol{v}$. For simplicity, we identify the vector $\boldsymbol{v}$ and a sequence $v(n)$

satisfying $v(n) = v_n$ for $0 \leq n < N$ and $v(n) = 0$ otherwise. The concatenation of M vectors $\boldsymbol{v}_m$, $0 \leq m < M$, is denoted by $(\boldsymbol{v}_0\ \boldsymbol{v}_1 \cdots \boldsymbol{v}_{M-1})$ or $(\boldsymbol{v}_m)_{m=0}^{M-1}$. A matrix is denoted by a bold uppercase letter and an $M \times N$ matrix $\boldsymbol{A}$ with its entries as $\boldsymbol{A} = \left[a_n^{(m)}\right]_{m=0,n=0}^{M-1,N-1}$. The mth row and the nth column vectors of $\boldsymbol{A}$ are denoted by $\boldsymbol{a}^m$ and $\boldsymbol{a}_n$, respectively. Moreover, $\boldsymbol{A}^*$ and $\boldsymbol{A}^H$ denote the complex conjugate and Hermitian transpose of $\boldsymbol{A}$, respectively. The determinant and rank of $\boldsymbol{A}$ are denoted by $\det(\boldsymbol{A})$ and $\mathrm{rank}(\boldsymbol{A})$, respectively. Consider $\boldsymbol{f}_N^i$ to be the ith row of the N-dimensional DFT matrix $\boldsymbol{F}_N = [W_N^{mn}]_{m=0,n=0}^{N-1,N-1}$ with $W_N = \exp(-2j\pi/N)$ and $\boldsymbol{h}_N^i$ be the ith row of the N-dimensional WH matrix $\boldsymbol{H}_N$, whose recursive generation is given by

$$\boldsymbol{H}_{2^m} = \begin{bmatrix} \boldsymbol{H}_{2^{m-1}} & \boldsymbol{H}_{2^{m-1}} \\ \boldsymbol{H}_{2^{m-1}} & -\boldsymbol{H}_{2^{m-1}} \end{bmatrix},$$

for $\boldsymbol{H}_1 = [1]$. An indexed set resembles a set of numbered elements and is denoted by outline $\mathbb{S} = \{s_n\}_{n=0}^{N-1}$ while a family $\mathcal{S}$ stands for a collection of sets. $\delta(\tau)$ represents *Kronecker's delta function* and $[x]_L$ denotes a non-negative integer that is less than L and satisfies $(x - [x]_L) \bmod L = 0$. For an integer m, $\boldsymbol{m}_2$ denotes the binary extension of m and $\boldsymbol{m}_2 \oplus \boldsymbol{n}_2$ represents the bit-wise exclusive OR logic of two binary vectors $\boldsymbol{m}_2$ and $\boldsymbol{n}_2$. The expectation operation of a random variable x is denoted as $E\{x\}$.

II. Preliminary

Here, a set $\mathbb{S} = \{\boldsymbol{s}_n\}_{n=0}^{N-1}$ consisting of N length-L sequences an (N, L)-SS is introduced, denoted by (N, L)-$\mathbb{S}$, while a set $\mathcal{S} = \{\mathbb{S}^m\}_{m=0}^{M-1}$ comprising M (N, L)-SSs is called an (M, N, L)-*sequence family* (SQF) and denoted by (M, N, L)-$\mathcal{S}$.

For two sequences $\boldsymbol{s}$ of length L and $\boldsymbol{s}'$ of length L', their corresponding *aperiodic convolution* and *aperiodic correlation* [2] are defined as follows :

$$\psi_{\mathrm{A}}(\boldsymbol{s}, \boldsymbol{s}'; \tau) := \sum_{\ell=0}^{L-1} s(\ell) s'(\tau - \ell), \tag{1}$$

$$\phi_{\mathrm{A}}(\boldsymbol{s}, \boldsymbol{s}'; \tau) := \sum_{\ell=0}^{L-1} s(\ell) \left[s'(\tau + \ell)\right]^*. \tag{2}$$

If $\boldsymbol{s} = \boldsymbol{s}'$, $\phi_{\mathrm{A}}(\boldsymbol{s}, \boldsymbol{s}'; \tau)$ in (2), then it is called the *auto-correlation* of $\boldsymbol{s}$ and is denoted as $\phi_{\mathrm{A}}(\boldsymbol{s}; \tau)$. Otherwise, it is called the *cross-correlation* between $\boldsymbol{s}$ and $\boldsymbol{s}'$. Since $\phi_{\mathrm{A}}(\boldsymbol{s}, \boldsymbol{s}'; \tau)$ takes non-zero values on the interval $-L' < \tau < L$, to coordinate with the convolution given in (1), and we define two length-$(L + L' - 1)$ vectors as follows:

$$\begin{aligned} \boldsymbol{\psi}_{\mathrm{A}}(\boldsymbol{s}, \boldsymbol{s}') &:= (\psi_{\mathrm{A}}(\boldsymbol{s}, \boldsymbol{s}'; \tau))_{\tau=0}^{L+L'-2}, \\ \underline{\boldsymbol{\phi}}_{\mathrm{A}}(\boldsymbol{s}, \boldsymbol{s}') &:= (\phi_{\mathrm{A}}(\boldsymbol{s}, \boldsymbol{s}'; -\tau))_{\tau=-L'+1}^{L-1}. \end{aligned} \tag{3}$$

Notice that the τth entry of $\underline{\boldsymbol{\phi}}_{\mathrm{A}}(\boldsymbol{s}, \boldsymbol{s}')$ is given by $\underline{\phi}_{\mathrm{A}}(\boldsymbol{s}, \boldsymbol{s}'; \tau) = \phi_{\mathrm{A}}(\boldsymbol{s}, \boldsymbol{s}; 1 - \tau - L')$ and we proved the following equalities in Appendix A.

$$\boldsymbol{\psi}_{\mathrm{A}}\left(\boldsymbol{s}, \boldsymbol{\psi}_{\mathrm{A}}(\boldsymbol{s}', \boldsymbol{s}'')\right) = \boldsymbol{\psi}_{\mathrm{A}}\left(\boldsymbol{\psi}_{\mathrm{A}}(\boldsymbol{s}, \boldsymbol{s}'), \boldsymbol{s}''\right), \tag{4}$$

$$\boldsymbol{\psi}_{\mathrm{A}}\left(\boldsymbol{s}, \underline{\boldsymbol{\phi}}_{\mathrm{A}}(\boldsymbol{s}', \boldsymbol{s}'')\right) = \underline{\boldsymbol{\phi}}_{\mathrm{A}}\left(\boldsymbol{\psi}_{\mathrm{A}}(\boldsymbol{s}, \boldsymbol{s}'), \boldsymbol{s}''\right). \tag{5}$$

For two sequences $\boldsymbol{s}$ and $\boldsymbol{s}'$ of length-L, the *periodic convolution* and *periodic correlation* are defined as follows:

$$\begin{aligned} \psi_{\mathrm{P}}(\boldsymbol{s}, \boldsymbol{s}'; \tau) &:= \sum_{\ell=0}^{L-1} s(\ell) s'([\tau - \ell]_L) \\ &= \sum_{\ell=0}^{L-1} s([\tau - \ell]_L) s'(\ell), \end{aligned} \tag{6}$$

$$\begin{aligned} \phi_{\mathrm{P}}(\boldsymbol{s}, \boldsymbol{s}'; \tau) &:= \sum_{\ell=0}^{L-1} s(\ell) \left[s'([\ell + \tau]_L)\right]^* \\ &= \sum_{\ell=0}^{L-1} s([\ell - \tau]_L) \left[s'(\ell)\right]^*. \end{aligned} \tag{7}$$

For the case $\tau \geq 0$, the periodic convolution and correlation are related with the aperiodic convolution and correlation, respectively, as

$$\psi_{\mathrm{P}}(\boldsymbol{s}, \boldsymbol{s}'; \tau) = \psi_{\mathrm{A}}(\boldsymbol{s}, \boldsymbol{s}'; \tau) + \psi_{\mathrm{A}}(\boldsymbol{s}, \boldsymbol{s}'; \tau + L) \tag{8}$$

$$\phi_{\mathrm{P}}(\boldsymbol{s}, \boldsymbol{s}'; \tau) = \phi_{\mathrm{A}}(\boldsymbol{s}, \boldsymbol{s}'; \tau) + (1 - \delta(\tau))\, \phi_{\mathrm{A}}(\boldsymbol{s}, \boldsymbol{s}'; \tau - L) \tag{9}$$

Similar to the aperiodic case, if we define length-L vectors as

$$\begin{aligned} \boldsymbol{\psi}_{\mathrm{P}}(\boldsymbol{s}, \boldsymbol{s}') &:= (\psi_{\mathrm{P}}(\boldsymbol{s}, \boldsymbol{s}'; \tau))_{\tau=0}^{L-1}, \\ \underline{\boldsymbol{\phi}}_{\mathrm{P}}(\boldsymbol{s}, \boldsymbol{s}') &:= (\phi_{\mathrm{P}}(\boldsymbol{s}, \boldsymbol{s}'; -\tau))_{\tau=0}^{L-1}, \end{aligned} \tag{10}$$

it is not difficult to observe that the following equalities

$$\boldsymbol{\psi}_{\mathrm{P}}\left(\boldsymbol{s}, \boldsymbol{\psi}_{\mathrm{P}}(\boldsymbol{s}', \boldsymbol{s}'')\right) = \boldsymbol{\psi}_{\mathrm{P}}\left(\boldsymbol{\psi}_{\mathrm{P}}(\boldsymbol{s}, \boldsymbol{s}'), \boldsymbol{s}''\right), \tag{11}$$

$$\boldsymbol{\psi}_{\mathrm{P}}\left(\boldsymbol{s}, \underline{\boldsymbol{\phi}}_{\mathrm{P}}(\boldsymbol{s}', \boldsymbol{s}'')\right) = \underline{\boldsymbol{\phi}}_{\mathrm{P}}\left(\boldsymbol{\psi}_{\mathrm{P}}(\boldsymbol{s}, \boldsymbol{s}'), \boldsymbol{s}''\right), \tag{12}$$

hold for sequences $\boldsymbol{s}$, $\boldsymbol{s}'$, and $\boldsymbol{s}''$ of the same length.

For a length L sequence $\boldsymbol{s}$, let $\mathscr{S}^e[\boldsymbol{s}] := (s([e + \ell]_L))_{\ell=0}^{L-1}$ be the e-shifted sequence of $\boldsymbol{s}$. Then, we obtain the following form:

$$\begin{aligned} &\phi_{\mathrm{P}}(\mathscr{S}^e[\boldsymbol{s}], \mathscr{S}^{e'}[\boldsymbol{s}]; \tau) \\ =&\sum_{\ell=0}^{L-1} s([e + \ell]_L) s^*([e' + \tau + \ell]_L) \\ =&\phi_{\mathrm{P}}(\boldsymbol{s}; e' - e + \tau). \end{aligned} \tag{13}$$

For two SSs, (N, L)-$\mathbb{S}$ and (N, L')-$\mathbb{S}'$, the *aperiodic correlation sum* can be defined as

$$\Phi_{\mathrm{A}}\left(\mathbb{S}, \mathbb{S}'; \tau\right) := \sum_{n=0}^{N-1} \phi_{\mathrm{A}}(\boldsymbol{s}_n, \boldsymbol{s}'_n; \tau). \tag{14}$$

If $\mathbb{S} = \mathbb{S}'$, it is called the *aperiodic auto-correlation sum* and is denoted by $\Phi_{\mathrm{A}}\left(\mathbb{S}; \tau\right)$. Otherwise, (14) is called the *aperiodic cross-correlation sum*.

A. ZCZ-SS

Definition 1. A sequence $\boldsymbol{s}$ is called the *perfect sequence* (PS) if the periodic auto-correlation of $\boldsymbol{s}$ is zero except for zero-shift, *i.e.*, $\phi_{\mathrm{P}}(\boldsymbol{s}; \tau) = E_{\boldsymbol{s}} \delta(\tau)$, where $E_{\boldsymbol{s}} := \boldsymbol{s}\boldsymbol{s}^H$. From (13), each shifted version of a PS $\mathscr{S}^e[\boldsymbol{s}]$, $0 \leq e < L$, is also PS.

Chu-sequence [28] generated by

$$s(\ell)=\begin{cases}W_{2L}^{-Q\ell^2} & \text{even } L,\\ W_{2L}^{-Q\ell(\ell+1)} & \text{odd } L,\end{cases} \tag{15}$$

is a well-known polyphase PS, where Q resembles an integer relatively prime to L and, in this study, we let $Q=1$ for simplicity.

Meanwhile, $\boldsymbol{a}$ is considered as the M-sequence of length-L, that is, a binary sequence with the periodic auto-correlation function

$$\phi_{\mathrm{P}}(\boldsymbol{a};\tau)=\begin{cases}L; & \tau=0,\\ -1; & \text{otherwise.}\end{cases}$$

Subsequently, the two real-valued sequence generated by

$$s(\ell)=a(\ell)+\frac{-1\pm\sqrt{L+1}}{L}, \tag{16}$$

is the PS called the *modified maximum-length* sequence [35].

Definition 2. An (M,L)-$\mathbb{S}$ is called a ZCZ-SS, and it is denoted by $(M,L;Z)$-ZCZ, if the periodic auto-correlation of each sequence is zero for $0<|\tau|\le Z$ and the periodic cross-correlation between any distinct sequence pair is zero for $|\tau|\le Z$, *i.e.*,

$$\phi_{\mathrm{P}}(\boldsymbol{s}^m,\boldsymbol{s}^{m'};\tau)=E_{\boldsymbol{s}^m}\delta(m-m')\delta(\tau),\quad |\tau|\le Z. \tag{17}$$

Then, each $(M,L;Z)$-ZCZ satisfies $Z\le\lfloor L/M\rfloor-1$ [36]. However, the equality may not be achieved for a ZCZ-SS with a small alphabet size and the bound is considered as $Z\le\lfloor L/2M\rfloor$ for binary ZCZ-SS.

For a PS $\boldsymbol{s}$ of length-L, let $Z=\lfloor\frac{L}{M}\rfloor-1$, then the SS constructed by

$$\mathbb{S}'=\left\{\mathscr{S}^{m(Z+1)}[\boldsymbol{s}]\right\}_{m=0}^{M-1}, \tag{18}$$

is an $(M,L;Z)$-ZCZ.

Example 1. When $Q=1$, the length-8 Chu-sequence generated using (15) is

$$\boldsymbol{s}=\left(W_{16}^0,W_{16}^{15},W_{16}^{12},-W_{16}^{15},W_{16}^0,-W_{16}^{15},W_{16}^{12},W_{16}^{15}\right).$$

For the case of $M=2$, the length of ZCZ is $Z=8/2-1=3$, and from (18), the SS $\mathbb{S}'=\left\{\mathscr{S}^0[\boldsymbol{s}],\mathscr{S}^4[\boldsymbol{s}]\right\}$ with sequences

$$\begin{cases}\mathscr{S}^0[\boldsymbol{s}]=\left(W_{16}^0,W_{16}^{15},W_{16}^{12},-W_{16}^{15},W_{16}^0,-W_{16}^{15},W_{16}^{12},W_{16}^{15}\right),\\ \mathscr{S}^4[\boldsymbol{s}]=\left(W_{16}^0,-W_{16}^{15},W_{16}^{12},W_{16}^{15},W_{16}^0,W_{16}^{15},W_{16}^{12},-W_{16}^{15}\right),\end{cases} \tag{19}$$

is $(2,8;3)$-ZCZ.

Meanwhile, from the length-7 M-sequence $\boldsymbol{a}=(-\,-\,+\,+\,+\,-\,+)$, the PS generated using (16) is $\boldsymbol{s}=(-0.74,-0.74,1.26,1.26,1.26,-0.74,1.26)$. For $M=2$, we have $Z=2$ for this case and the SS $\mathbb{S}'=\left\{\mathscr{S}^0[\boldsymbol{s}],\mathscr{S}^3[\boldsymbol{s}]\right\}$ with sequences

$$\begin{cases}\mathscr{S}^0[\boldsymbol{s}'] &=(-0.74,-0.74,1.26,1.26,1.26,-0.74,1.26),\\ \mathscr{S}^3[\boldsymbol{s}'] &=(1.26,1.26,-0.74,1.26,-0.74,-0.74,1.26),\end{cases} \tag{20}$$

is $(2,7;2)$-ZCZ.

B. Concatenative Complete Complementary Codes

Definition 3. An (N,L)-SS $\mathbb{C}=\{\boldsymbol{c}_n\}_{n=0}^{N-1}$ is known as a *complementary* SS if the auto-correlation sum of $\mathbb{C}$ is zero except for zero-shift, *i.e.*, $\Phi_{\mathrm{A}}(\mathbb{C};\tau)=E_{\mathbb{C}}\delta(\tau)$, where $E_{\mathbb{C}}=\sum_{n=0}^{N-1}E_{\boldsymbol{c}_n}$. In addition, an (M,N,L)-SQF $\mathcal{C}=\{\mathbb{C}^m\}_{m=0}^{M-1}$ is called a *complete complementary code* (CCC), denoted by (M,N,L)-CCC, if the sequences in each row are complementary SS and the cross-correlation sum between any two distinct complementary SSs is zero for all shifts, *i.e.*,

$$\Phi_{\mathrm{A}}(\mathbb{C}^m,\mathbb{C}^{m'};\tau)=NL\delta(m-m')\delta(\tau). \tag{21}$$

For a given (M,N,L)-CCC $\mathcal{C}=\{\mathbb{C}^m\}_{m=0}^{M-1}$, where $\mathbb{C}^m=\{\boldsymbol{c}_n^m\}_{n=0}^{N-1}$, if the (M,NL)-SS generated by concatenating the sequences in each complementary SS, *i.e.*,

$$\mathbb{S}=\{\boldsymbol{s}^m\}_{m=0}^{M-1},\quad \boldsymbol{s}^m=(\boldsymbol{c}_n^m)_{n=0}^{N-1}, \tag{22}$$

is $(M,NL;Z)$-ZCZ, then we call $\mathcal{C}$ *Concatenative* CCC (CCCC) and denote it as $(M,N,L;Z)$-CCCC.

To describe the constructions proposed in [32] in a unified manner, we let $\boldsymbol{\Omega}=\boldsymbol{H}_N$ for binary CCCC construction while for polyphase case $\boldsymbol{\Omega}=\boldsymbol{F}_N$ and $\boldsymbol{\omega}^k$ be the kth row of $\boldsymbol{\Omega}$. Now, let $\mathcal{C}=\left\{\left\{\boldsymbol{\omega}^k\right\}_{n=0}^{N-1}\right\}_{m=0}^{N-1}$ with the interleavring rule $k=\pi^{(m)}(n)$ be the (N,N,N)-SQF comprising the rows of $\boldsymbol{\Omega}$. Subsequently, if we use an unexacting expression $k=\boldsymbol{k}_2$ for binary case and specify the interleaving rule as follows:

$$k=\pi^{(m)}(n)=\begin{cases}\boldsymbol{m}_2\oplus\boldsymbol{n}_2 & \text{for binary,}\\ [m+n]_N & \text{for polyphase,}\end{cases} \tag{23}$$

then the resultant SQFs are the binary $(N,N,N;N/2)$-CCCC and polyphase $(N,N,N;N-1)$-CCCC. Notice the interleaving rule given in (23) can be deinterleaved by

$$n=\bar{\pi}^{(m)}(k)=\begin{cases}\boldsymbol{k}_2\oplus\boldsymbol{m}_2 & \text{for binary,}\\ [k-m]_N & \text{for polyphase,}\end{cases} \tag{24}$$

and the proposed constructions are optimal in the sense that the qualities on the (conjectured) bounds, $Z=N-1$ and $N/2$ respectively, hold for both cases. In the practical applications of $(N,N,L;Z)$-CCCC, a large merit figure $\eta=(Z+1)/L\le 1$ is expected to achieve a high SE and we may improve it by ZP scheme [32].

Example 2. Consider $M=N=4$ and consider the binary case with the indexes in the binary forms, *i.e.*, $0=[00]_2$, $1=[01]_2$, $2=[10]_2$, $3=[11]_2$. If we then carry out the additions of indexes over the extended Galois field GF(2^2), *e.g.*, $2\oplus 3=[10]_2\oplus[11]_2=[01]_2=1$, we obtain

$$\mathcal{C}=\left\{\begin{array}{cccc}\boldsymbol{h}_4^0 & \boldsymbol{h}_4^1 & \boldsymbol{h}_4^2 & \boldsymbol{h}_4^3\\ \boldsymbol{h}_4^1 & \boldsymbol{h}_4^0 & \boldsymbol{h}_4^3 & \boldsymbol{h}_4^2\\ \boldsymbol{h}_4^2 & \boldsymbol{h}_4^3 & \boldsymbol{h}_4^0 & \boldsymbol{h}_4^1\\ \boldsymbol{h}_4^3 & \boldsymbol{h}_4^2 & \boldsymbol{h}_4^1 & \boldsymbol{h}_4^0\end{array}\right\}, \tag{25}$$

while the polyphase CCCC

$$\mathcal{C}=\left\{\begin{array}{cccc}\boldsymbol{f}_4^0 & \boldsymbol{f}_4^1 & \boldsymbol{f}_4^2 & \boldsymbol{f}_4^3\\ \boldsymbol{f}_4^1 & \boldsymbol{f}_4^2 & \boldsymbol{f}_4^3 & \boldsymbol{f}_4^0\\ \boldsymbol{f}_4^2 & \boldsymbol{f}_4^3 & \boldsymbol{f}_4^0 & \boldsymbol{f}_4^1\\ \boldsymbol{f}_4^3 & \boldsymbol{f}_4^0 & \boldsymbol{f}_4^1 & \boldsymbol{f}_4^2\end{array}\right\},$$

can be constructed with the natural addition for indexes. Although the resultant CCCCs are of the same length $L = N = 4$, the ZCZ of the binary CCCC is $Z = 2$ while it is increased to $Z = 3$ for the polyphase case. Accordingly, the SS constructed by (22) is a (4,16;2)-ZCZ with merit figure $\eta = 2/3$. However, if we terminate $\mathbf{0}_2$ for each sequence before concatenation as

$$\mathbb{S} = \left\{ \begin{array}{c} \boldsymbol{s}^0 \\ \boldsymbol{s}^1 \\ \boldsymbol{s}^2 \\ \boldsymbol{s}^3 \end{array} \right\} = \left\{ \begin{array}{c} \left(\boldsymbol{h}_4^0\ \mathbf{0}_2\ \boldsymbol{h}_4^1\ \mathbf{0}_2\ \boldsymbol{h}_4^2\ \mathbf{0}_2\ \boldsymbol{h}_4^3\ \mathbf{0}_2\right) \\ \left(\boldsymbol{h}_4^1\ \mathbf{0}_2\ \boldsymbol{h}_4^0\ \mathbf{0}_2\ \boldsymbol{h}_4^3\ \mathbf{0}_2\ \boldsymbol{h}_4^2\ \mathbf{0}_2\right) \\ \left(\boldsymbol{h}_4^2\ \mathbf{0}_2\ \boldsymbol{h}_4^3\ \mathbf{0}_2\ \boldsymbol{h}_4^0\ \mathbf{0}_2\ \boldsymbol{h}_4^1\ \mathbf{0}_2\right) \\ \left(\boldsymbol{h}_4^3\ \mathbf{0}_2\ \boldsymbol{h}_4^2\ \mathbf{0}_2\ \boldsymbol{h}_4^1\ \mathbf{0}_2\ \boldsymbol{h}_4^0\ \mathbf{0}_2\right) \end{array} \right\}, \quad (26)$$

then the resultant SS is a (4,24;4)-ZCZ with a improved merit figure $\eta = 4/5$.

III. Brief Review of CC-CDMA and CS-CDMA

We consider the down-link of M users in MA systems equipped with single transmitting/receiving antenna. For the sake of establishing a unifying description, let $\boldsymbol{u}^m$, $0 \le m < M$, be the mth user's modulated symbol vector[1] of length-K selected from constellation $\mathcal{S}^K$, and we assume that the antenna transmits the elements of $\vec{\boldsymbol{x}}$ serially. We consider the general case that users are distributed on the distinct positions and the mth user receives the transmitted signal over length-$(P^{(m)}+1)$ quasi-static multipath channel $\boldsymbol{h}_P^m = \left[h^{(m)}(p)\right]_{p=0}^{P^{(m)}}$ for $E\left\{h^{(m)}(p)\left(h^{(m)}(p')\right)^*\right\} = \sigma_p^2\delta(p-p')$. Thus, the received signal can be expressed as follows:

$$\vec{\boldsymbol{y}}^m = \boldsymbol{\psi}_{\mathrm{A}}\left(\boldsymbol{h}_P^m, \vec{\boldsymbol{x}}\right) + \vec{\boldsymbol{\xi}}^m,$$

where $\vec{\boldsymbol{\xi}}^m$ denotes the mutually independent circularly symmetric *additive white Gaussian noise* (AWGN) with zero mean and variance $E\left\{\vec{\xi}_\ell^{(m)}\left(\vec{\xi}_{\ell'}^{(m)}\right)^*\right\} = \sigma^2\delta(\ell-\ell')$. In the present analysis, we let $\max_{0\le m<M}\left\{P^{(m)}\right\} \le G$ and assume the mth user's CIR $\boldsymbol{h}_P^m$ can be perfectly recovered at the receiver of the mth user.

A. Review of CC-CDMA [14]

Fig. 1 illustrates the tranceiver structure of CC-CDMA. Let $\mathcal{C} = \{\mathbb{C}^m\}_{m=0}^{M-1}$ be an (M, N, L)-CCC. In CC-CDMA, the mth CS-SS $\mathbb{C}^m = \{\boldsymbol{c}_n^m\}_{n=0}^{N-1}$ is assigned as the mth user's spreading SS, and all user's modulated symbols are transmitted by packets, each of which comprises N sub-packets. In the nth sub-packet, the mth user's modulated symbol vector $\boldsymbol{u}^m$ is convolutionally spread by the nth spreading sequence $\boldsymbol{c}_n^m$ as $\boldsymbol{x}_n^m = \boldsymbol{\psi}_{\mathrm{A}}(\boldsymbol{u}^m, \boldsymbol{c}_n^m)$ to yield the signal-part of length-$(K+L-1)$ of the nth sub-packet. To combat multi-path interference, guard-part $\mathbf{0}_G$ is padded on the tail of the signal-part to yield the nth sub-packet and, by concatenating these sub-packets, we generate the mth user's packet $\boldsymbol{x}^m = (\boldsymbol{x}_n^m\ \mathbf{0}_G)_{n=0}^{N-1}$ of length-$(N(K+L+G-1))$. Finally, all user's packets are summarized together as $\vec{\boldsymbol{x}} = \sum_{m=0}^{M-1}\boldsymbol{x}^m$ and sent to the transmitting antenna.

[1]Even the lengths of the user's symbol vector are not necessarily the same in some cases, but we assume equal length for simplicity.

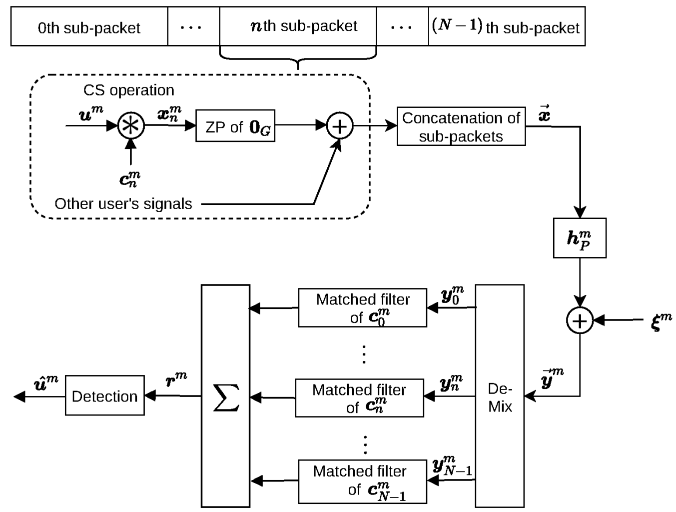

Fig. 1. Down-link system model of CC-CDMA

Owing to the guard-part $\mathbf{0}_G$, from the received signal, we can obtain N inter-sub-packet interference free vectors of length-$\left(K+L+P^{(m)}-1\right)$ as

$$\begin{aligned}\boldsymbol{y}_n^m &= \left(\vec{y}^{(m)}(n(K+L+G-1)+\ell)\right)_{\ell=0}^{K+L+P^{(m)}-2} \\ &= \boldsymbol{\psi}_{\mathrm{A}}\left(\boldsymbol{h}_P^m, \boldsymbol{x}_n\right) + \boldsymbol{\xi}_n^m, \end{aligned} \quad (27)$$

for $0 \le n < N$, where we let $\boldsymbol{x}_n := \sum_{m=0}^{M-1}\boldsymbol{x}_n^m$ and $\boldsymbol{\xi}_n^m := \left(\vec{\xi}^{(m)}(n(K+L+G-1)+\ell)\right)_{\ell=0}^{K+L+P^{(m)}-2}$. Each $\boldsymbol{y}_n^m$ is then inputed into the matched filter of the corresponding spreading sequence $\boldsymbol{c}_n^m$ and the outputs of matched filter can be summarized as follows:

$$\underline{\boldsymbol{r}}^m = \sum_{n=0}^{N-1}\underline{\boldsymbol{\phi}}_{\mathrm{A}}(\boldsymbol{y}_n^m, \boldsymbol{c}_n^m). \quad (28)$$

We proved in Appendix B that the CC-CDMA provides ICI-free relationship as

$$\boldsymbol{r}^m = E\boldsymbol{\psi}_{\mathrm{A}}\left(\boldsymbol{h}_P^m, \boldsymbol{u}^m\right) + \boldsymbol{\eta}^m, \quad (29)$$

where $\boldsymbol{r}^m = \left(\underline{r}^{(m)}(\tau)\right)_{\tau=L-1}^{K+P^{(m)}+L-2}$, $E = LN$, and $\boldsymbol{\eta}^m$ denotes a length-$(K+P^{(m)})$ complex Gasussian random vector with zero mean and variance $E\left\{(\boldsymbol{\eta}^m)^H\boldsymbol{\eta}^m\right\} = E\sigma^2\boldsymbol{I}_{K+P^{(m)}}$.

B. Review of CS-CDMA [23]

Fig. 2 illustrates the downlink transceiver structure of CS-CDMA. In CS-CDMA, the mth sequence of an $(M, L; Z)$-ZCZ $\mathbb{S} = \{\boldsymbol{s}^m\}_{m=0}^{M-1}$, satisfying $Z \ge K+G-1$, is assigned as the mth user's spreading sequence. At the transmitter, the zero vector $\mathbf{0}_{L-K}$ is padded on the tail of $\boldsymbol{u}^m$ to yield the signal vector $\boldsymbol{d}^m = [\boldsymbol{u}^m, \mathbf{0}_{L-K}]$ of length L. Subsequently, the periodic convolutions $\boldsymbol{x}^m = \boldsymbol{\psi}_{\mathrm{P}}(\boldsymbol{d}^m, \boldsymbol{s}^m)$ are calculated between $\boldsymbol{d}^m$ and $\boldsymbol{s}^m$ as CS operation and the resultant signals are summarized with other signals as $\boldsymbol{x} = \sum_{m=0}^{M-1}\boldsymbol{x}^m$. Eventually,

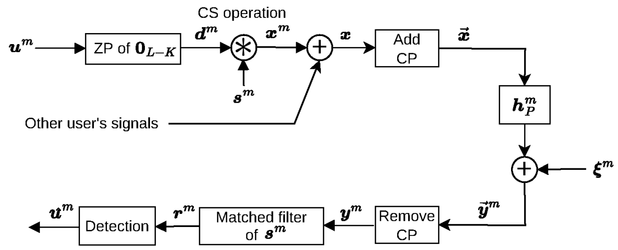

Fig. 2. Down-link system model of CS-CDMA

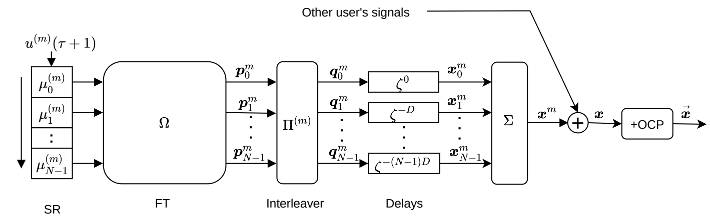

Fig. 3. FT-based transmitter implementation for CCC-CDMA

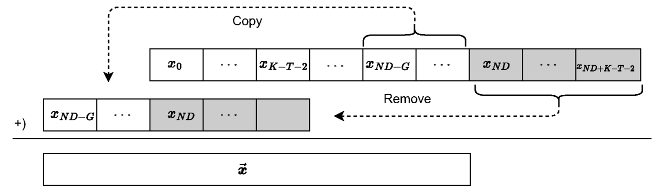

Fig. 4. Operation of OCP

after adding length-G CP, the signal $\vec{\boldsymbol{x}} = [\boldsymbol{x}(L-G : L-1), \boldsymbol{x}]$ is sent to the antenna of the transmitter.

Let $\boldsymbol{y}^m$ be the mth user's CP removed signal of length L. As despreading process of CS, we then calculate the periodic cross-correlation between the received signal $\boldsymbol{y}$ and the mth user's spreading sequence $\boldsymbol{s}^m$ as $\underline{\boldsymbol{r}}^m = \underline{\phi}_{\mathrm{P}}(\boldsymbol{y}^m, \boldsymbol{s}^m)$ and detect the transmitted symbols from the first $K + P^{(m)}$ output $\boldsymbol{r}^m = \left(\underline{r}^{(m)}(\tau)\right)_{\tau=0}^{K+P^{(m)}-1}$. In Appendix C, we proved that if we let $E = E_{\boldsymbol{s}^m}$, then CS-CDMA provides the same relationship given in (29).

C. The comparison of CC- and CS-CDMAs

The CC- and CS-CDMAs provide the same ICI-free input-output relationship and achieves higher SE than the DS-CDMAs employing Gold sequence, M-sequence, and Walsh sequence [18], [19], [37], [38]. When comparing the SEs of these two systems, CC-CDMA transmits KM symbols using packet of length $N(K+L+G-1)$, where the number of users is bounded by $M \leq N$. Accordingly, the SE of CC-CDMA is bounded by

$$\eta_{\mathrm{CC}} \leq \frac{K}{K+G+L_C-1}, \tag{30}$$

where L_C denotes the length of each sequence.

Meanwhile, for CS-CDMA, to transmit K symbols for each user, it is necessary to employ a ZCZ-SS of length $L \geq M(Z+1)$, where $Z \geq K+G-1$. Accordingly, the length of packet is $L+G \geq M(K+G)+G$ and the SE of CS-CDMA is bounded by

$$\eta_{\mathrm{CS}} \leq \frac{K}{K+G+G/M}. \tag{31}$$

When comparing (30) with (31), CS-CDMA achieves higher efficiency than CC-CDMA in the case $M(L_C-1) > G$ and vise versa. Additionally, a large L allows $K \gg G$ and the SE of CC- and CS-CDMAs are close to that of OFDMA given by $\eta_{\mathrm{OFDMA}} = K/(K+G)$.

IV. CCC-CDMA WITH ITS IMPLEMENTATIONS

In this section, we introduce interleaver/deinterleaver components and propose a novel comprehensive FT-based implementation structure for CCC-CDMA.

A. FT-based tranceiver structures of CCC-CDMA

The FT-based transmitter structure of CCC-CDMA is illustrated in Fig. 3. $\boldsymbol{\mu}^m(\tau)$ denotes the state of the mth user's *shift-register* (SR) of length N at time τ and we assume that the initial states are set to $\mathbf{0}_N$ for all users. Subsequently, the modulated symbols are serially fed into SR and, after each shift, the N-points FT is performed over SR to yield signal $\boldsymbol{\mu}^m(\tau)\boldsymbol{\Omega}$ until all modulated symbols are shifted out from the SR. Consequently, the transmitter performs totally $K+N-1$ FTs, that begins and terminates at the states $\boldsymbol{\mu}^m(0) = \left(u^{(m)}(0), \mathbf{0}_{N-1}\right)$ and $\boldsymbol{\mu}^m(K+N-1) = \left(\mathbf{0}_{N-1}, u^{(m)}(K-1)\right)$, respectively.

Let $p_k^{(m)}(\tau)$ represent the kth output of FT at time τ and let $\boldsymbol{p}_k^m := \left(p_k^{(m)}(\tau)\right)_{\tau=0}^{K+N-1}$. With the mth user's interleaver $\Pi^{(m)}$ whose interleaving rule $n = \pi^{(m)}(k)$ is specified by (24), $\boldsymbol{q}_n^m$ is inputed into the delay ζ^{-nD} for $D = N+T$ to yield $\boldsymbol{x}_n = \left(\mathbf{0}_{nD}, \boldsymbol{q}_n, \mathbf{0}_{(N-n-1)D}\right)_{n=0}^{N-1}$ and the delayed signals are summarized to yield the mth user's signal vector $\boldsymbol{x}^m = (\boldsymbol{x}_n^m)_{n=0}^{N-1}$. The resultant signal is then added with other signals as $\boldsymbol{x} = \sum_{m=0}^{M-1} \boldsymbol{x}^m$. Finally, the length-$(K+G-T-1)$ vector $\boldsymbol{x}(ND-G : ND+K-T-2)$, called the *overlapped CP* (OCP), is appended to the head of signal $\boldsymbol{x}$ to yield the signal $\vec{\boldsymbol{x}}$, where the length-$(K-T-1)$ signal $\boldsymbol{x}(ND : ND+K-T-2)$ is removed from the tail and summarized with $\boldsymbol{x}(0 : K-T-2)$ while signal $\boldsymbol{x}(ND-G : ND-1)$ with length-G is copied to the head of $\boldsymbol{x}$, as illustrated in Fig. 4. Notice that the former overlapped part convert aperiodic convolution to periodic one according to (9) while the later CP part acts as guard against multipath.

At the mth user's receiver, after the removal of CP, the length-ND vector $\boldsymbol{y}^m$ is arranged into a *cyclic shift-register* (CSR) whose tth value at time τ can be expressed by $\nu_t^{(m)}(\tau) = y^{(m)}([t-\tau]_{ND})$. The D spaced CSR $\nu_{nD}^{(m)}(\tau)$, $0 \leq d < N$, are connected to the deinterleaver $\bar{\Pi}^{(m)}$ and the nDth CSR $\nu_{nD}^{(m)}(\tau)$ is inputed into the kth input of the FT $v_k^{(m)}(\tau)$ with the deinterleaving rule $k = \pi^{(m)}(n)$ specified by (24). Let $\boldsymbol{v}^m(\tau) := \left(v_k^{(m)}(\tau)\right)_{k=0}^{N-1}$. The N points transform

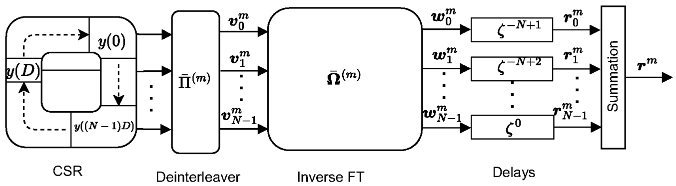

Fig. 5. FT-based receiver implementation of CCC-CDMA

is then performed over the outputs of the deinterleaver as $\boldsymbol{w}^m(\tau) = \boldsymbol{v}^m(\tau)\bar{\boldsymbol{\Omega}}$ and the resultant signal is inputed to delay $\zeta^{-[-n-1]_N}$ to yield $\boldsymbol{r}_n^m = (\boldsymbol{0}_n, \boldsymbol{w}_n^m, \boldsymbol{0}_{N-n-1})_{n=0}^{N-1}$. Lastly, we detect the transmitted data based on the summarized vector $\boldsymbol{r}^m = \sum_{n=0}^{N-1} \boldsymbol{r}_n^m$.

B. Example

For sake of simplicity, we consider two users case that the base station spreads $\boldsymbol{u}^0 = (1, -1, 1, -1)$ and $\boldsymbol{u}^1 = (1, 1, -1, 1)$ using $\boldsymbol{s}^0$ and $\boldsymbol{s}^1$ shown in (26), respectively. Then, it is not difficult to see that CS-CDMA results

$$\begin{aligned} \boldsymbol{x}^0 &= (0, 0, 1, 0, -1, 0, 0, -2, 3, -4, 3, -2, \\ &\quad 2, 0, -1, 0, -1, 0, 2, -2, 1, 0, -1, 2), \\ \boldsymbol{x}^1 &= (0, 0, -1, 2, -3, 2, 0, 2, 1, 2, 1, 0, \\ &\quad 2, 0, -3, 2, 1, -2, 2, 2, -1, -2, 1, 0), \end{aligned} \tag{32}$$

and the signal sent to transmitting antenna can be represented as follows:

$$\begin{aligned} \vec{\boldsymbol{x}} &= (2, 0, 0, 0, 2, -4, 2, 0, 0, 4, -2, 4, \\ &\quad -2, 4, 0, -4, 2, 0, -2, 4, 0, 0, -2, 0, 2). \end{aligned} \tag{33}$$

On the other hand, for the proposed transmitter shown in Fig. 3, we have $\boldsymbol{q}_0^0 = \boldsymbol{p}_0^0 = (1, 0, 1, 0, -1, 0, -1)$, $\boldsymbol{q}_1^0 = \boldsymbol{p}_1^0 = (1, -2, 3, -4, 3, -2, 1)$, $\boldsymbol{q}_2^0 = \boldsymbol{p}_2^0 = (1, 0, -1, 0, -1, 0, 1$, and $\boldsymbol{q}_3^0 = \boldsymbol{p}_3^0 = (1, -2, 1, 0, -1, 2, -1)$ for the 0th user while the outputs of the 1th user are $\boldsymbol{q}_0^1 = \boldsymbol{p}_1^1 = (1, 0, -1, 2, -3, 2, -1)$, $\boldsymbol{q}_1^1 = \boldsymbol{p}_0^1 = (1, 2, 1, 2, 1, 0, 1)$, $\boldsymbol{q}_2^1 = \boldsymbol{p}_3^1 = (1, 0, -3, 2, 1, -2, 1)$, and $\boldsymbol{q}_3^1 = \boldsymbol{p}_2^1 = (1, 2, -1, -2, 1, 0, -1)$. From $K = 4$ and $T = 2$, we derive $D = 6$, and $\boldsymbol{x}^0$ and $\boldsymbol{x}^1$ in Fig. 3 are as follows:

$$\begin{aligned} \boldsymbol{x}^0 &= (1, 0, 1, 0, -1, 0, 0, -2, 3, -4, 3, -2, \\ &\quad 2, 0, -1, 0, -1, 0, 2, -2, 1, 0, -1, 2, -1), \\ \boldsymbol{x}^1 &= (1, 0, -1, 2, -3, 2, 0, 2, 1, 2, 1, 0, \\ &\quad 2, 0, -3, 2, 1, -2, 2, 2, -1, -2, 1, 0, -1). \end{aligned} \tag{34}$$

After summation of $\boldsymbol{x}^0$ and $\boldsymbol{x}^1$, we can obtain the signal in (33) by OCP operation for $G = 1$ and $K - T - 1 = 1$.

Assuming ideal channel, the signal of the CSR in 5 at $\tau = 0$ can be expressed as

$$\begin{aligned} \boldsymbol{y} &= (\underline{0}, 0, 0, 2, -4, 2, \underline{0}, 0, 4, -2, 4, -2, \\ &\quad \underline{4}, 0, -4, 2, 0, -2, \underline{4}, 0, 0, -2, 0, 2). \end{aligned} \tag{35}$$

Performing the FT over the positions marked in underline, the 0th user obtains the signals $\boldsymbol{w}_0^0 = (8, 0, 0, 0, 0, 0, 8, 0)$, $\boldsymbol{w}_1^0 = (0, 0, -8, 8, -8, 0, 0, 0)$, $\boldsymbol{w}_2^0 = (-8, 0, 8, 0, 0, 0, 0, 0)$, and $\boldsymbol{w}_3^0 = (0, 0, 0, 0, -8, 8, -8, 0)$. Summation after corresponding delays, the 0th user obtains $\boldsymbol{r}^0 = (0, -8, 0, 16, -16, 16, -16, 0, 0, 8, 0)$ and recovers the modulated symbols from $(16, -16, 16, -16, 0)$.

C. The proof of equivalence

While the ZCZ-SS generated from CCCC is employed for CS-CDMA, we proved in Appendix D that the outputs at the transmitter and receiver of the mth user are represented by

$$\begin{aligned} & x_{\text{CS}}^{(m)}(\tau) \\ &= \sum_{n=0}^{N-1} \sum_{\ell=0}^{N-1} u^{(m)}([\tau - \ell - nD]_{ND}) c_n^{(m)}(\ell), \end{aligned} \tag{36}$$

$$\begin{aligned} & \underline{r}_{\text{CS}}^{(m)}(\tau) \\ &= \sum_{\ell=0}^{L-1} \sum_{n=0}^{N-1} y^{(m)}([-\tau - \ell - nD]_{ND}) \left[c_n^{(m)}(\ell)\right]^*, \end{aligned} \tag{37}$$

respectively.

In the FT-based transmitter structure, since the value of the ℓth SR at time τ is given by $\mu_\ell^{(m)}(\tau) = u^{(m)}(\tau - \ell)$, the kth output of the FT can be expressed as

$$\begin{aligned} p_k^{(m)}(\tau) &= \sum_{\ell=0}^{N-1} \mu_\ell^{(m)}(\tau) \omega_k^{(\ell)} \\ &= \sum_{\ell=0}^{N-1} u^{(m)}(\tau - \ell) \omega_k^{(\ell)}, \end{aligned} \tag{38}$$

while the mth user's signal at time τ is represented by

$$x^{(m)}(\tau) = \sum_{n=0}^{N-1} x_n^{(m)}(\tau) = \sum_{n=0}^{N-1} q_n^{(m)}(\tau - nD). \tag{39}$$

Since the nth input of the delay is connected with the kth output of FT by interleaving rule $k = \pi^{(m)}(n)$, substituting (38) into (39), we obtain

$$\begin{aligned} x^{(m)}(\tau) &= \sum_{n=0}^{N-1} p_{\pi^{(m)}(n)}^{(m)}(\tau - nD) \\ &= \sum_{n=0}^{N-1} \sum_{\ell=0}^{N-1} u^{(m)}(\tau - \ell - nD) \, \omega_{\pi^{(m)}(n)}^{(\ell)} \\ &= \sum_{n=0}^{N-1} \sum_{\ell=0}^{N-1} u^{(m)}(\tau - \ell - nD) \, \omega_\ell^{\left(\pi^{(m)}(n)\right)}, \end{aligned} \tag{40}$$

where the last equality is caused by the symmetry of $\boldsymbol{\Omega}$. Thus, if the interleaving rule is specified using (23), the mth user's output can be expressed as

$$x^{(m)}(\tau) = \sum_{n=0}^{N-1} \sum_{\ell=0}^{N-1} u^{(m)}(\tau - \ell - nD) \, c_n^{(m)}(\ell). \tag{41}$$

Let $\tau = n'D + \ell'$ for $0 \le n' < N$ and $0 \le \ell' < D$. Resultantly, since $u^{(m)}(\tau) = 0$ if $\tau < 0$ or $\tau \ge K$, (40) can be rewritten for the case $n' > 0$ as

$$\begin{aligned} & x_{\mathrm{CS}}^{(m)}(\tau) \\ =& \sum_{n=0}^{N-1}\sum_{\ell=0}^{N-1} u^{(m)}\left([(n'-n)D + (\ell'-\ell)]_{ND}\right) c_n^{(m)}(\ell) \\ =& \sum_{\ell=0}^{\ell'} u^{(m)}(\ell'-\ell)\, c_{n'}^{(m)}(\ell) + \sum_{\ell=\ell'}^{N-1} u^{(m)}(D+\ell'-\ell)\, c_{n'-1}^{(m)}(\ell) \\ =& x^{(m)}(\tau), \end{aligned} \tag{42}$$

and for the case $n' = 0$ as

$$\begin{aligned} & x_{\mathrm{CS}}^{(m)}(\tau) \\ =& \sum_{\ell=0}^{\ell'} u^{(m)}(\ell'-\ell)\, c_0^{(m)}(\ell) + \sum_{\ell=\ell'}^{N-1} u^{(m)}(D+\ell'-\ell)\, c_{N-1}^{(m)}(\ell) \\ =& x^{(m)}(\tau) + x^{(m)}(L+\tau). \end{aligned} \tag{43}$$

Thus, it is not difficult to observe that in Fig. 4, the summation of the overlapped part realize (43), while (42) guarantees that the copied part comprises the CP of CS-CDMA. Moreover, since it is common for all users, the OCP can be processed after the summation of all user's signals.

In the proposed receiver structure, since the kth output of the interleaver at time τ can be expressed as $v_k^{(m)}(\tau) = y^{(m)}([nD-\tau]_{ND})$, for $n = \bar{\pi}^{(m)}(k)$, the ℓth output of the FT is given by

$$\begin{aligned} w_\ell^{(m)}(\tau) &= \sum_{k=0}^{N-1} v_k^{(m)}(\tau)\bar{\omega}_\ell^{(k)} \\ &= \sum_{n=0}^{N-1} y^{(m)}\left([nD-\tau]_{ND}\right)\bar{\omega}_\ell^{\left(\bar{\pi}^{(m)}(n)\right)}, \end{aligned} \tag{44}$$

and, from $r_\ell^{(m)}(\tau) = w_\ell^{(m)}(\tau + \ell + 1 - N)$, we obtain

$$\begin{aligned} & r^{(m)}(\tau - N + 1) \\ =& \sum_{\ell=0}^{N-1} w_\ell^{(m)}(\tau+\ell) \\ =& \sum_{n'=0}^{N-1}\sum_{\ell=0}^{N-1} y^{(m)}\left([n'D-\tau-\ell]_{ND}\right)\bar{\omega}_\ell^{\left(\bar{\pi}^{(m)}(n')\right)} \\ =& \sum_{n=0}^{N-1}\sum_{\ell=0}^{N-1} y^{(m)}\left([-\tau-\ell-nD]_{ND}\right)\bar{\omega}_\ell^{\left(\bar{\pi}^{(m)}([-n]_N)\right)}, \end{aligned} \tag{45}$$

where we let $n = [-n']_N$ for the last equation.

Now, let $\bar{\mathbf{\Omega}} = \left[h_\ell^{([-k]_N)}\right]_{k=0,\ell=0}^{N-1,N-1}$ or $\boldsymbol{F}_N^{-1}$ for binary or polyphase cases, respectively. Then, we have

$$\bar{\omega}_\ell^{\left(\bar{\pi}^{(m)}([-n]_N)\right)} = \begin{cases} h_\ell^{(\boldsymbol{m}_2\oplus\boldsymbol{n}_2)} = c_n^{(m)}(\ell) & \text{for binary,} \\ W_N^{-(m+n)\ell} = \left[c_n^{(m)}(\ell)\right]^* & \text{for polyphase,} \end{cases} \tag{46}$$

and since all elements of the binary CCCC are real values, the output of (45) coincides with (37).

V. PERFORMANCE ANALYSIS OF CCC-CDMA

In this section, we evaluate *bit error rate* (BER) for systems having the input-output relationship defined in (29) and evaluate the computational complexities required for CCC-CDMA. We assume that ML detection is employed at the receiver and, for the sake of notational simplicity, in the following, we omit the user index m.

A. Upper-Bound on BER over Rayleigh fading channels

We first consider the *pair-wise error probability* (PEP) that the transmitted symbol vector $\boldsymbol{u}$ is erroneously detected into $\hat{\boldsymbol{u}}$. Accordingly, the conditional PEP is upper bounded as

$$\begin{aligned} & P\left(\boldsymbol{u} \to \hat{\boldsymbol{u}} \,|\boldsymbol{h}_P\right) \\ \le& \Pr\left\{\|\boldsymbol{r} - E\boldsymbol{\psi}_{\mathrm{A}}(\boldsymbol{h}_P, \boldsymbol{u})\|^2 \ge \|\boldsymbol{r} - E\boldsymbol{\psi}_{\mathrm{A}}(\boldsymbol{h}_P, \hat{\boldsymbol{u}})\|^2 \,|\boldsymbol{h}_P\right\} \\ =& \Pr\left\{2\Re\left\{\boldsymbol{eH\eta}^H\right\} \le -\|\boldsymbol{eH}\|^2 \,|\boldsymbol{h}_P\right\}, \end{aligned} \tag{47}$$

where $\boldsymbol{e} := \boldsymbol{u} - \hat{\boldsymbol{u}}$ and $\boldsymbol{H}$ denotes the Teoplitz matrix of size $K \times (K+P)$ given by

$$\boldsymbol{H} = \left(\left[\left(\mathscr{S}^{-k}\left[\bar{\boldsymbol{h}}\right]\right)^T\right]_{k=0}^{K-1}\right)^T,$$

where $\bar{\boldsymbol{h}} = [\boldsymbol{h}_P \ \boldsymbol{0}_{K-1}]$.

Since $\boldsymbol{\eta}$ in (29) is composed of the Gaussian random variables with zero mean and variance N_0, $\boldsymbol{H\eta}^H$ is also a Gaussian vector with zero mean and covariance matrix $E\{\boldsymbol{H\eta}^H\boldsymbol{\eta H}^H\} = N_0\boldsymbol{I}_K$. Consequently, $\Re\left\{\boldsymbol{eH\eta}^H\right\}$ contains the Gaussian distribution with mean zero and variance $D\left(\Re\left\{\boldsymbol{eH\eta}^H\right\}\right) = \frac{N_0}{2}\|\boldsymbol{eH}\|^2$ and the conditional PEP is upper-bounded as follows:

$$P\left(\boldsymbol{e}\,|\boldsymbol{h}_P\right) \le \mathcal{Q}\left(\sqrt{\frac{\|\boldsymbol{eH}\|^2}{2N_0}}\right) = \mathcal{Q}\left(\sqrt{\frac{\|\boldsymbol{h}_P\boldsymbol{E}\|^2}{2N_0}}\right), \tag{48}$$

where $\mathcal{Q}(x)$ denotes the Gaussian Q-function and $\boldsymbol{E}$ represents the Teoplitz matrix of size $(P+1) \times (K+P)$ can be expressed using $\bar{\boldsymbol{e}} = [\boldsymbol{e} \ \boldsymbol{0}_P]$ as follows:

$$\boldsymbol{E} = \left(\left[\left(\mathscr{S}^{-p}\left[\bar{\boldsymbol{e}}\right]\right)^T\right]_{p=0}^{P}\right)^T. \tag{49}$$

Notice that $\boldsymbol{xE} = \boldsymbol{0}_{K+P}$ has solution if and only if $\boldsymbol{x} = \boldsymbol{0}_{P+1}$ and hence, $\mathrm{rank}(\boldsymbol{E}) = P+1$.

From Craig's representation [39] (also see [40]), the bound described in (48) is written as

$$P\left(\boldsymbol{e}\,|\boldsymbol{h}_P\right) \le \frac{1}{\pi}\int_0^{\frac{\pi}{2}} \exp\left\{-\frac{\|\boldsymbol{h}_P\boldsymbol{E}\|^2}{4N_0\sin^2\alpha}\right\} d\alpha. \tag{50}$$

Since the channel is assumed to subject quasi-static uncorrelated multipath Rayleigh fading, $\boldsymbol{h}_P$ consists of mutually independent Gaussian random variable with zero mean and variance $E\{\boldsymbol{h}_P^H\boldsymbol{h}_P\} = \boldsymbol{\Sigma}_P := \mathrm{diag}[\sigma_0^2, \sigma_1^2, \cdots, \sigma_P^2]$, where we assume $\sigma_p > 0$, $p = 0, 1, \cdots, P$, for simplicity.

Subsequently, since $\boldsymbol{h}_P$ has the *probability density function* given by

$$f_{\boldsymbol{h}_P}(\boldsymbol{x}) = \frac{\exp\left(-\boldsymbol{x}\boldsymbol{\Sigma}_P^{-1}\boldsymbol{x}^H\right)}{\pi^{P+1}\det(\boldsymbol{\Sigma}_P)}, \tag{51}$$

the (unconditional) PEP is bounded by

$$P(\boldsymbol{e}) = \int P(\boldsymbol{e}|\boldsymbol{x}) f_{\boldsymbol{h}_P}(\boldsymbol{x}) d\boldsymbol{x} \leq \frac{1}{\pi} \int_0^{\frac{\pi}{2}} \frac{(4N_0)^{P+1} \sin^{2(P+1)} \alpha}{\det(\boldsymbol{B}\boldsymbol{\Sigma}_P)} \, d\alpha, \quad (52)$$

where $\boldsymbol{B} = \|\boldsymbol{E}\|^2 + 4N_0 \left(\sin^2 \alpha\right) \boldsymbol{\Sigma}_P^{-1}$. Since $\boldsymbol{\Sigma}_P$ is a non-negative diagonal matrix and $\|\boldsymbol{E}\|^2 = [\phi_A(\boldsymbol{e}, i-j)]_{i=0,j=0}^{P,P}$ is the auto-correlation matrix of $\boldsymbol{e}$, which is a non-negative definite Hermitian matrix. Thus, we have $\det(\boldsymbol{B}) \geq \det\left(\|\boldsymbol{E}\|^2\right)$, and PEP is bounded as

$$P(\boldsymbol{e}) \leq \frac{C(P+1)}{\det(\|\boldsymbol{E}\|^2)}, \quad (53)$$

where for a positive integer x, we let

$$C(x) = \frac{(4N_0)^x}{\pi \det(\boldsymbol{\Sigma}_x)} \int_0^{\pi/2} \sin^{2x} \alpha \, d\alpha = \frac{{}_{2x-1}C_{x-1} N_0^x}{\det(\boldsymbol{\Sigma}_x)}, \quad (54)$$

for the binomial coefficient ${}_nC_r$. The right-hand side of bound (53) is finite if and only if $\det\left(\|\boldsymbol{E}\|^2\right) \neq 0$, that is, $\operatorname{rank}\left(\|\boldsymbol{E}\|^2\right) = P+1$. Accordingly, if the input-output relationship is given by (29) over the length-$(P+1)$ multipath Reyleigh fading channel, then such systems provide the full path diversity of order $P+1$.

Let $\mathcal{E}(\boldsymbol{u}) = \mathcal{E}(u_0) \times \cdots \times \mathcal{E}(u_{K-1})$ and $\mathcal{E} := \cup_{u \in \mathcal{S}} \mathcal{E}(u)$, where $\mathcal{E}(u) := \{e = u - \hat{u}\}_{\hat{u} \in \mathcal{S}}$ for each $u \in \mathcal{S}$. (see details in [41].) Then, BER is given by

$$\text{BER} = \frac{1}{K \log_2 |\mathcal{S}|} \sum_{\boldsymbol{e} \in \mathcal{E}^K - \{\boldsymbol{0}_K\}} n_b(\boldsymbol{e}) \sum_{\boldsymbol{u} \in \mathcal{S}^K; \boldsymbol{e} \in \mathcal{E}(\boldsymbol{u})} P(\boldsymbol{e}), \quad (55)$$

where $n_b(\boldsymbol{e})$ is the number of bit errors involved by $\boldsymbol{e}$ and it can be simplified to

$$\text{BER} = \frac{1}{K} \sum_{\boldsymbol{e} \in \mathcal{E}^K - \{\boldsymbol{0}_K\}} \frac{w(\boldsymbol{e}) P(\boldsymbol{e})}{|\mathcal{S}|^{w(\boldsymbol{e})}}, \quad (56)$$

for BPSK and QPSK modulations, where $w(\boldsymbol{e}) := \|\boldsymbol{e}\|^2/4$ denotes normalized weight of $\boldsymbol{e}$.

B. Complexity

We first consider the computational complexity in terms of the complex multiplications required for the CS operation. While an $(N, N, N; Z)$-CCCC is employed in the CCC-CDMA, the conventional CC- and CS-CDMAs require complex multiplications of order $\mathcal{O}(N^2)$ to spread a modulated symbol. In the proposed FT-based structure, the number of multiplications required for spreading a modulated symbol is order of $\mathcal{O}\left(\frac{(K+N)N}{K} \log_2 N\right)$, primarily because the size-N FFT is performed as $(K+N-1) \approx K+N$ times. Thus, for the case $K \gg N$, the polyphase CCC-CDMA has a complexity of order $\mathcal{O}(N \log_2 N)$, less than that of OFDM(A) $\mathcal{O}(\log_2 K)$. Moreover, the binary CCC-CDMA completely eliminates the multiplications in CS operation at the expense of SE.

Considering the channel equalization complexity, OFMD(A) provides the ML detection with a single tap equalization. For CCC-CDMA, on the other hand, we may recover the transmitted symbols under the ML criterion using the Viterbi algorithm. To detect a transmitted symbol, we need to compare metrics for at least $|\mathcal{S}|^P$ states, each of which requires a complex multiplication [42]. Thus, overall complexity of CCC-CDMA $\mathcal{O}(N \log_2 N) + \mathcal{O}(|\mathcal{S}|^P)$ is much higher than that of OFDM(A) $\mathcal{O}(\log_2 K)$ especially for a high order modulation and under a large multipath environment. Although we may achieve a certain diversity order by employing a low complexity equalizer such as the frequency domain linear equalizer proposed in [43], in this paper, we limit our discussions and performance evaluations for the receiver under the ML criterion.

VI. Simulation Results

We have shown in the previous section that, the performance of systems that provide the input-output relationship shown in (29) over Rayleigh fading multipath channel does not depend on the sequence selection. Hence, the binary and polyphase CCCCs, Chu-ZCZs, and M-ZCZs with the same SF achieve the same performance. Thus, in this study, we evaluate the resistances against clipping noise and Doppler frequency shifts. For CCCCs, the resistance against clipping noise is considered to monotonically weaken with the increment of padding zeros [33] and, in this study, we only test the crude CCCCs.

The evaluations are executed by computer simulations over four paths ($P = 3$) Rayleigh fading channel with uniformly distributed PDP for the cases of CCCC, Chu-ZCZ, and OFDMA of lengths $L = 256/1024$ while $L = 255/1023$ for M-ZCZ. For each case, we assumed $M = N$ users transmit QPSK modulated symbols of the same length-$(N/2 - P + 1)$ per packet, which is the maximum length of the binary CCCC that provides the lowest SE. Thus, for the CCCCs, Chu-ZCZ, and OFDMA, $M = N = \sqrt{L} = 16$ and 32 for $L = 256$ and 1024, respectively, while the lengths of the corresponding QPSK symbol vectors are 6 and 14, respectively, and these are 1 symbol short for M-ZCZ. We also normalized the *power delay profile* (PDP) to $\sum_{p=0}^{P} \sigma_p^2 = 1$. Therefore, at both the transmitter and receiver, the *signal to noise ratio* (SNR) can be expressed by $\bar{E}_{\boldsymbol{x}}/\sigma^2$, where $\bar{E}_{\boldsymbol{x}} = E_{\boldsymbol{x}}/L$ denotes the average transmission energy. At the receiver, the ML with Viterbi algorithm is utilized to recover the transmitted symbols, and we plotted each BER point after accumulating over $5,000$ bit errors.

A. Clipping resistances

In Fig. 6, we plotted the SNR vs. BER over the quasi-static Rayleigh fading channel for two clipping levels: $\text{PAPR}_0 = 2$ dB and 4 dB. Under the assumption that polar clipping occurs at the transmitters, we replaced the signal $\boldsymbol{x}$ by $\boldsymbol{x}'$ as

$$x'(\ell) = \begin{cases} x(\ell), & |x(\ell)|^2 \leq E_{\text{th}}, \\ \frac{\sqrt{E_{\text{th}}}}{|x(\ell)|} x(\ell), & |x(\ell)|^2 > E_{\text{th}}, \end{cases}$$

where $E_{\text{th}} = \bar{E}_{\boldsymbol{x}} \times \text{PAPR}_0$ denotes the clipping threshold and detected the transmitted symbols based on the ML criterion with the perfect CIR at all receivers.

This article has been accepted for publication in IEEE Transactions on Wireless Communications. This is the author's version which has not been fully edited and content may change prior to final publication. Citation information: DOI 10.1109/TWC.2023.3250659

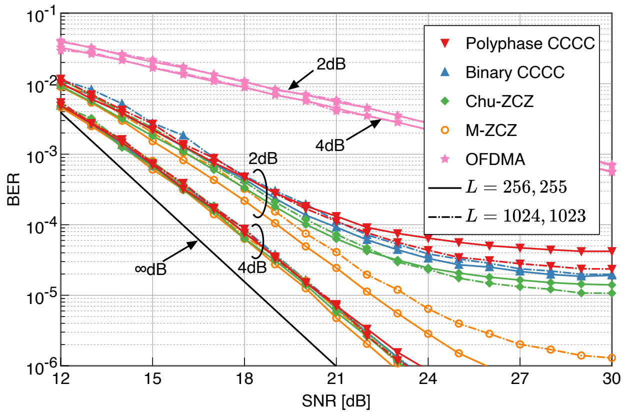

Fig. 6. Comparison of clipping resistances over 4-paths fading channel

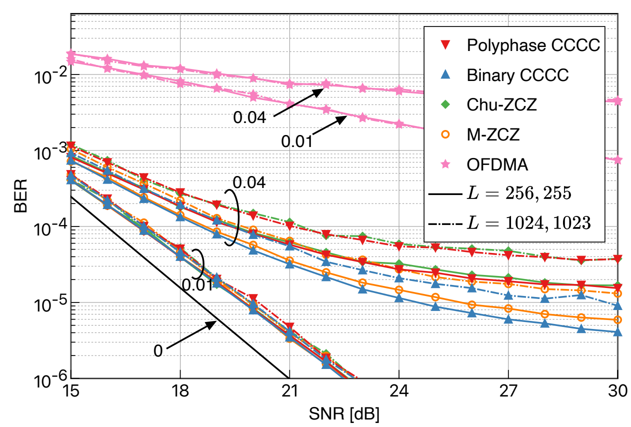

Fig. 8. Comparison of Doppler resistances

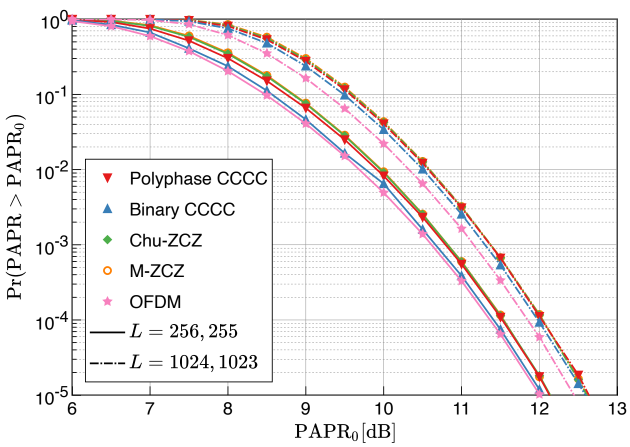

Fig. 7. Comparison of PAPR distributions

We can observe from Fig. 6 that, as indicated in [27], the best performances are achieved by M-ZCZ for all cases and their BER curves exhibit full path diversity without any error floors. Meanwhile, OFDMA exhibits the worst performance for all cases owing to a lack in diversity order while error floors are appeared in the BER curves of CCCCs and Chu-ZCZ. Evidently, Fig. 6 also indicates that the lengthening employed sequence enhances the robustness against clipping noise with a higher SE, it is a simple but efficient countermeasure to mitigate the influence of clipping noise.

To explain the effect of SF, in Fig. 7, we plotted $\Pr\{\text{PAPR} > \text{PAPR}_0\}$, the *complementary cumulative probability function* of $\text{PAPR} := \max_{\ell=0}^{L-1}\left\{|x(\ell)|^2\right\}/\bar{E}_{\boldsymbol{x}}$ after testing 10^8 packets. It is evident from the figure that, the curves of the polyphase CCCC-ZCZ, Chu-ZCZ, and M-ZCZ with the same length overlap each other and hence the occurrence probabilities of them are almost identical. Thus, the difference in distribution of the despread clipping noise causes different tolerances and it has the minimum energy for the white Gaussian distribution. Thus, M-ZCZ constructed from a PR sequence has the best resistance, and despite the fact that the enlargement of SF increases the probability of clipping, the resistance against clipping noise is enhanced with a large SF because the distribution of the despread clipping noise for these cases is close to the white Gaussian and we may benefit from processing gain. When comparing the Chu-ZCZ of the same length, although CCCC has higher error floor level, the low complexity implementation of CCC-CDMA enables easy enlargement of SF to combat clipping noise.

B. Doppler resistance

Under the assumption of a carrier frequency of 2 GHz and symbol duration $T_s = 100\ \mu s$, in Fig. 8, we compared BER performances over the fast fading channels with normalized maximum Doppler frequencies $f_{\max}T_s = 0.04, 0.01$, corresponding to moving velocities $f_{\max}T_s$ are 216 km/h, 54 km/h, respectively. The time varying channel was generated based on Jakes model [44] and we used the Rayleigh fading simulation model given in [45]. At the receiver, the ML detection was utilized with imperfect CIR information, *i.e.*, the CIR at each begin of packet was used for ML detection.

When comparing the curves of the case $f_{\max}T_s = 0.04$, the binary CCCC appears to be more resistant than M-ZCZ against fast fading and the polyphase sequences exhibit a similar weakness. In fact, over the fast fading channel, the M-ZCZ and binary CCCC disperse ICIs over all users with similar strengths while the polyphase sequences concentrate them on few neighboring channels. Thus, for the polyphase sequences, a sophisticatedly designed channel estimation and equalization can be employed to mitigate the ICI caused over fast fading channels.

VII. Conclusion

This study presented CCC-CDMA with its comprehensive FT-based implementation structure of the transceiver to reduce the computational complexity of CS operation. Simulation results show that the enlargement of SF strengthens the clipping resistance and the binary CCC-CDMA exhibits excellent robustness against Doppler frequency shifts.

This article has been accepted for publication in IEEE Transactions on Wireless Communications. This is the author's version which has not been fully edited and content may change prior to final publication. Citation information: DOI 10.1109/TWC.2023.3250659

ACKNOWLEDGMENT

The author would like to thank Bohulu Kwame Ackah for his help and support in completing this study. This work was supported by JSPS KAKENHI Grant Numbers JP16K06339.

APPENDIX

A. The proofs of (4) and (5)

The τth entry of the left-hand side of (4) can be calculated as

$$\begin{aligned}&\psi_{\mathrm{A}}\left(\boldsymbol{s},\boldsymbol{\psi}_{\mathrm{A}}(\boldsymbol{s}',\boldsymbol{s}'');\tau\right)\\ =&\sum_{\ell=0}^{L-1} s(\ell)\psi_{\mathrm{A}}(\boldsymbol{s}',\boldsymbol{s}'';\tau-\ell)\\ =&\sum_{\ell=0}^{L-1}\sum_{\ell'=0}^{L'-1} s(\ell)s'(\ell')s''(\tau-\ell-\ell'),\end{aligned} \tag{57}$$

and it coincides with that of the right-hand side given by

$$\begin{aligned}&\psi_{\mathrm{A}}\left(\boldsymbol{\psi}_{\mathrm{A}}(\boldsymbol{s},\boldsymbol{s}'),\boldsymbol{s}'';\tau\right)\\ =&\sum_{k=0}^{L+L'-2}\psi_{\mathrm{A}}(\boldsymbol{s},\boldsymbol{s}';k)s''(\tau-k)\\ =&\sum_{\ell=0}^{L-1}\sum_{k=0}^{L+L'-2} s(\ell)s'(k-\ell)s''(\tau-k)\\ =&\sum_{\ell=0}^{L-1}\sum_{\ell'=0}^{L'-1} s(\ell)s'(\ell')s''(\tau-\ell-\ell'),\end{aligned} \tag{58}$$

where we let $k=\ell+\ell'$ and the fact $s'(\ell')=0$ for $\ell\geq L'$ is utilized in the last equation.

Similarly, the τth entries of the left- and right-hand sides of (5) are given by

$$\begin{aligned}&\psi_{\mathrm{A}}\left(\bar{\boldsymbol{s}},\underline{\boldsymbol{\phi}}_{\mathrm{A}}(\boldsymbol{s}',\boldsymbol{s}'');\tau\right)\\ =&\sum_{\ell=0}^{L-1} s(\ell)\underline{\phi}_{\mathrm{A}}(\boldsymbol{s}',\boldsymbol{s}'';\tau-\ell)]\\ =&\sum_{\ell=0}^{L-1} s(\ell)\phi_{\mathrm{A}}(\boldsymbol{s}',\boldsymbol{s}'';1-L''-\tau+\ell)]\\ =&\sum_{\ell=0}^{L-1}\sum_{\ell'=0}^{L'-1} s(\ell)s'(\ell')\left[s''(1-L''-\tau+\ell+\ell')\right]^*,\end{aligned} \tag{59}$$

and

$$\begin{aligned}&\underline{\phi}_{\mathrm{A}}\left(\boldsymbol{\psi}_{\mathrm{A}}(\boldsymbol{s},\boldsymbol{s}'),\boldsymbol{s}'';\tau\right)\\ =&\phi_{\mathrm{A}}\left(\boldsymbol{\psi}_{\mathrm{A}}(\boldsymbol{s},\boldsymbol{s}'),\boldsymbol{s}'';1-L''-\tau\right)\\ =&\sum_{k=0}^{L+L'-2}\psi_{\mathrm{A}}(\boldsymbol{s},\boldsymbol{s}';k)\left[s''(1-L''-\tau+k)\right]^*\\ =&\sum_{\ell=0}^{L-1}\sum_{k=0}^{L+L'-2} s(\ell)s'(k-\ell)\left[s''(1-L''-\tau+k\right]^*\\ =&\sum_{\ell=0}^{L-1}\sum_{\ell'=0}^{L'-1} s(\ell)s'(\ell')\left[s''(1-L''-\tau+\ell+\ell')\right]^*,\end{aligned} \tag{60}$$

respectively. Thus, equality (5) holds.

B. Input-output relationship of CC-CDMA

Since equation (28) can be expressed as

$$\begin{aligned}\underline{\boldsymbol{r}}^m &= \sum_{n=0}^{N-1}\underline{\boldsymbol{\phi}}_{\mathrm{A}}(\boldsymbol{y}_n,\boldsymbol{c}_n^m)\\ &= \sum_{n=0}^{N-1}\underline{\boldsymbol{\phi}}_{\mathrm{A}}\left(\boldsymbol{\psi}_{\mathrm{A}}\left(\boldsymbol{h}_P,\boldsymbol{x}_n\right),\boldsymbol{c}_n^m\right)+\underline{\boldsymbol{\eta}}^m,\end{aligned} \tag{61}$$

where $\underline{\boldsymbol{\eta}}^m=\sum_{n=0}^{N-1}\underline{\boldsymbol{\phi}}_{\mathrm{A}}(\boldsymbol{\xi}_n,\boldsymbol{c}_n^m)$. Thus, from (5), it can be further calculated as

$$\begin{aligned}&\underline{\boldsymbol{r}}^m\\ =&\sum_{n=0}^{N-1}\boldsymbol{\psi}_{\mathrm{A}}\left(\boldsymbol{h}_P,\underline{\boldsymbol{\phi}}_{\mathrm{A}}\left(\boldsymbol{x}_n,\boldsymbol{c}_n^m\right)\right)+\underline{\boldsymbol{\eta}}^m\\ =&\boldsymbol{\psi}_{\mathrm{A}}\left(\boldsymbol{h}_P,\sum_{n=0}^{N-1}\underline{\boldsymbol{\phi}}_{\mathrm{A}}(\boldsymbol{x}_n,\boldsymbol{c}_n^m)\right)+\underline{\boldsymbol{\eta}}^m\\ =&\boldsymbol{\psi}_{\mathrm{A}}\left(\boldsymbol{h}_P,\sum_{n=0}^{N-1}\underline{\boldsymbol{\phi}}_{\mathrm{A}}\left(\sum_{m'=0}^{M-1}\boldsymbol{x}_n^{m'},\boldsymbol{c}_n^m\right)\right)+\underline{\boldsymbol{\eta}}^m\\ =&\boldsymbol{\psi}_{\mathrm{A}}\left(\boldsymbol{h}_P,\sum_{n=0}^{N-1}\underline{\boldsymbol{\phi}}_{\mathrm{A}}\left(\sum_{m'=0}^{M-1}\boldsymbol{\psi}_{\mathrm{A}}\left(\boldsymbol{u}^{m'},\boldsymbol{c}_n^{m'}\right),\boldsymbol{c}_n^m\right)\right)+\underline{\boldsymbol{\eta}}^m\\ =&\boldsymbol{\psi}_{\mathrm{A}}\left(\boldsymbol{h}_P,\sum_{m'=0}^{M-1}\boldsymbol{\psi}_{\mathrm{A}}\left(\boldsymbol{u}^{m'},\sum_{n=0}^{N-1}\underline{\boldsymbol{\phi}}_{\mathrm{A}}\left(\boldsymbol{c}_n^{m'},\boldsymbol{c}_n^m\right)\right)\right)+\underline{\boldsymbol{\eta}}^m,\end{aligned} \tag{62}$$

where property (5) is utilized in the last equation and we notice that

$$\sum_{n=0}^{N-1}\underline{\phi}_{\mathrm{A}}(\boldsymbol{c}_n^{m'},\boldsymbol{c}_n^m;\tau)=LN\delta(m-m')\delta(-\tau-L+1),$$

holds from (21). Thus, if we let $\boldsymbol{r}^m=\left(\underline{r}^{(m)}(\tau)\right)_{\tau=L-1}^{K+P+L-2}$, the output can be expressed as follows:

$$\boldsymbol{r}^m=LN\boldsymbol{\psi}_{\mathrm{A}}\left(\boldsymbol{h}_P,\boldsymbol{u}^m\right)+\boldsymbol{\eta}^m, \tag{63}$$

where $\boldsymbol{\eta}=\left(\underline{\eta}^{(m)}(\tau)\right)_{\tau=L-1}^{K+P+L-2}$ is a Gaussian random vector with zero mean and covariance

$$\begin{aligned}&E\left\{\boldsymbol{\eta}^H\boldsymbol{\eta}\right\}\\ =&E\left\{\sum_{n=0}^{N-1}\sum_{n'=0}^{N-1}\underline{\boldsymbol{\phi}}_{\mathrm{A}}^H(\boldsymbol{\xi}_n,\boldsymbol{c}_n^m)\underline{\boldsymbol{\phi}}_{\mathrm{A}}(\boldsymbol{\xi}_{n'},\boldsymbol{c}_{n'}^m)\right\}\\ =&\left[\sum_{n,n'=0}^{N-1}\sum_{\ell,\ell'=0}^{K+L+G-2}E\left\{\xi_n^*(\ell)\xi_{n'}(\ell')\right\}\right.\\ &\left.\qquad Bc_n^m(-\tau+\ell)\left[c_{n'}^m(-\tau'+\ell')\right]^*\right]_{\tau,\tau'=0}^{K+P-1}\\ =&\sigma^2\left[\sum_{n=0}^{N-1}\sum_{\ell=0}^{K+L+G-2}c_n^m(-\tau+\ell)\left[c_n^m(-\tau'+\ell)\right]^*\right]_{\tau,\tau'=0}^{K+P-1}\\ =&\sigma^2\left[\sum_{n=0}^{N-1}\phi_{\mathrm{A}}(\boldsymbol{c}_n^m,\boldsymbol{c}_n^m;\tau-\tau')\right]_{\tau,\tau'=0}^{K+P-1}\\ =&NL\sigma^2\boldsymbol{I}_{K+P}.\end{aligned} \tag{64}$$

C. Input-output relationship of CS-CDMA

Since the CP removed signal can be expressed as $\boldsymbol{y} = \boldsymbol{\psi}_{\rm P}(\boldsymbol{h}, \boldsymbol{x}) + \boldsymbol{\xi}$ for $\boldsymbol{h} = (\boldsymbol{h}_P, \boldsymbol{0}_{L-P})$ and $\boldsymbol{\xi} = \left(\vec{\xi}(\ell)\right)_{\ell=G}^{G+L-1}$, the despread signal is given by

$$\begin{aligned}&\underline{\boldsymbol{r}}^m\\ =&\underline{\boldsymbol{\phi}}_{\rm P}(\boldsymbol{y}, \boldsymbol{s}^m)\\ =&\underline{\boldsymbol{\phi}}_{\rm P}\left(\boldsymbol{\psi}_{\rm P}\left(\boldsymbol{h}, \boldsymbol{x}\right), \boldsymbol{s}^m\right) + \underline{\boldsymbol{\eta}}^m\\ =&\boldsymbol{\psi}_{\rm P}\left(\boldsymbol{h}, \underline{\boldsymbol{\phi}}_{\rm P}\left(\sum_{m'=0}^{M-1}\boldsymbol{\psi}_{\rm P}\left(\boldsymbol{d}^{m'}, \boldsymbol{s}^{m'}\right), \boldsymbol{s}^m\right)\right) + \underline{\boldsymbol{\eta}}^m\\ =&\boldsymbol{\psi}_{\rm P}\left(\boldsymbol{h}, \sum_{m'=0}^{M-1}\boldsymbol{\psi}_{\rm P}\left(\boldsymbol{d}^{m'}, \underline{\boldsymbol{\phi}}_{\rm P}\left(\boldsymbol{s}^{m'}, \boldsymbol{s}^m\right)\right)\right) + \underline{\boldsymbol{\eta}}^m, \quad (65)\end{aligned}$$

where $\boldsymbol{\eta}^m = \underline{\boldsymbol{\phi}}_{\rm P}(\boldsymbol{\xi}, \boldsymbol{s}^m)$.

Let $\boldsymbol{r}^m = \left(\underline{r}^{(m)}(\ell)\right)_{\ell=0}^{K+P-1}$, for $K+P \le Z$. Then, from (17) we obtain

$$\begin{aligned}\boldsymbol{r}^m =&E_{\boldsymbol{s}^m}\left(\psi_{\rm P}\left(\boldsymbol{h}, \boldsymbol{d}^m; \tau\right)\right)_{\tau=0}^{K+P-1} + \boldsymbol{\eta}^m\\ =&E_{\boldsymbol{s}^m}\boldsymbol{\psi}_{\rm A}\left(\boldsymbol{h}_P, \boldsymbol{u}^m\right) + \boldsymbol{\eta}^m, \quad (66)\end{aligned}$$

where $\boldsymbol{\eta}^m = \left(\underline{\eta}^{(m)}(\ell)\right)_{\ell=0}^{K+P-1}$ is a Gaussian random vector with zero mean and covariance

$$\begin{aligned}&E\left\{\boldsymbol{\eta}^H\boldsymbol{\eta}\right\}\\ =&E\left\{\underline{\boldsymbol{\phi}}_{\rm P}^H(\boldsymbol{\xi}, \boldsymbol{s}^m)\underline{\boldsymbol{\phi}}_{\rm P}(\boldsymbol{\xi}, \boldsymbol{s}^m)\right\}\\ =&\left[\sum_{\ell,\ell'=0}^{K+P-1} E\left\{\xi^*(\ell)\xi(\ell')\right\}\right.\\ &\left. s^m([-\tau+\ell]_{K+P}) \quad \left[s^m([-\tau'+\ell']_{K+P})\right]^*\right]_{\tau,\tau'=0}^{K+P-1}\\ =&\sigma^2\left[\phi_{\rm P}(\boldsymbol{s}^m, \boldsymbol{s}^m; \tau-\tau')\right]_{\tau,\tau'=0}^{K+P-1}\\ =&E_{\boldsymbol{s}^m}\sigma^2\boldsymbol{I}_{K+P}. \quad (67)\end{aligned}$$

D. Signal representations of the CS-CDMA with CCCC

Since the mth CCCC-ZCZ is represented by $s^{(m)}(\ell) = \sum_{n=0}^{N-1} c_n^{(m)}(\ell - nD)$, the transmitted signal can be expressed as follows:

$$\begin{aligned}&x^{(m)}(\tau)\\ =&\psi_{\rm A}(\boldsymbol{d}^m, \boldsymbol{s}^m; \tau)\\ =&\sum_{n=0}^{N-1}\sum_{t=0}^{ND-1} u^{(m)}([\tau - t]_{ND})c_n^{(m)}(t - nD)\\ =&\sum_{n=0}^{N-1}\sum_{k=0}^{N-1}\sum_{\ell=0}^{D-1} u^{(m)}([\tau - \ell - kD]_{ND})c_n^{(m)}(\ell + (k-n)D)\\ =&\sum_{n=0}^{N-1}\sum_{\ell=0}^{N-1} u^{(m)}([\tau - \ell - nD]_{ND})c_n^{(m)}(\ell), \quad (68)\end{aligned}$$

where we let $t = kD + \ell$, for $0 \le k < N$ and $0 \le \ell < D$.

Similarly, the received signal can be expressed as

$$\begin{aligned}&\underline{r}^{(m)}(\tau)\\ =&\underline{\phi}_{\rm P}(\boldsymbol{y}, \boldsymbol{s}^m; \tau)\\ =&\phi_{\rm P}(\boldsymbol{y}, \boldsymbol{s}^m; -\tau)\\ =&\sum_{n=0}^{N-1}\sum_{t=0}^{ND-1} y([-\tau - t]_{ND})\left[c_n^{(m)}(t)\right]^*\\ =&\sum_{k=0}^{N-1}\sum_{\ell=0}^{D-1}\sum_{n=0}^{N-1} y([-\tau - \ell - kD]_{ND})\left[c_n^{(m)}(\ell + kD)\right]^* (69)\end{aligned}$$

and, substituting $c_n^{(m)}(\ell + kD) = \delta(k-n)c_n^{(m)}(\ell)$, it can be represented as

$$\underline{r}^{(m)}(\tau) = \sum_{\ell=0}^{D-1}\sum_{n=0}^{N-1} y([-\tau - \ell - nD]_{ND})\left[c_n^{(m)}(\ell)\right]^*. \quad (70)$$

References

[1] S. Verdú and S. Shamai(Shitz), "Spectral efficiency of CDMA with random spreading," *IEEE Trans. Inf. Theory*, vol. 45, no. 2, pp. 622–640, Mar. 1999.

[2] P. Z. Fan and M. Darnell, *Sequence Design for Communications Applications*. John Wiley & Sons Inc., 1996.

[3] J. A. C. Bingham, "Multicarrier modulation for data transmission: An idea whose time has come," *IEEE Commun. Mag.*, vol. 28, pp. 5–14, May 1990.

[4] A. N. Akansu, O. Duhamel, X. Liu, and M. de Courville, "Orthogonal transmultiplexers in communications: A review," *IEEE Trans. Signal Process.*, vol. 46, no. 4, pp. 979–995, Apr. 1998.

[5] C. Han and T. Hashimoto, "Almost linear interleaver and its application in coded OFDM over Rayleigh fading channel," in *Proc. IEEE Int. Symp. Personal, Indoor and Mobile Radio Commun. (PIMRC'13)*, London, U.K., Sep. 2013, pp. 687–692.

[6] ——. (2021, Jun.) Performance enhanced coded OFDM with almost linear interleaver over rayleigh fading channels. [Online]. Available: https://doi.org/10.36227/techrxiv.14740899.v2

[7] N. Suehiro and M. Hatori, "N-shift cross-orthogonal sequences," *IEEE Trans. Inf. Theory*, vol. IT-34, no. 1, pp. 143–146, Jan. 1988.

[8] C. Han, N. Suehiro, and T. Hashimoto, "A systematic framework for the construction of optimal complete complementary codes," *IEEE Trans. Inf. Theory*, vol. 57, no. 9, pp. 6033–6042, Sep. 2011.

[9] B. Shen, Y. Yang, Y. Feng, and Z. Zhou, "A generalized construction of mutually orthogonal complementary sequence sets with non-power-of-two lengths," *IEEE Transactions on Communications*, vol. 69, no. 7, pp. 4247–4253, 2021.

[10] Z. Wang, D. Ma, G. Gong, and E. Xue, "New construction of complementary sequence (or array) sets and complete complementary codes," *IEEE Transactions on Information Theory*, vol. 67, no. 7, pp. 4902–4928, 2021.

[11] N. Suehiro, "A signal design without co-channel interference for approximately synchronized cdma systems," *IEEE J. Sel. Areas Commun.*, vol. 12, no. 5, pp. 837–841, Jun. 1994.

[12] C. Han, T. Hashimoto, and N. Suehiro, "A new construction method of zero-correlation zone sequences based on complete complementary codes," *IEICE Trans. Found.*, vol. E91-A, no. 12, pp. 3698–3702, Dec. 2008.

[13] Z. Zhou, D. Zhang, T. Helleseth, and J. Wen, "A construction of multiple optimal zcz sequence sets with good cross correlation," *IEEE Transactions on Information Theory*, vol. 64, no. 2, pp. 1340–1346, 2018.

[14] N. Suehiro and N. Kuroyanagi, "Multipath-tolerant binary signal design for approximately synchronized CDMA systems without co-channel interference using complete complementary codes," in *Proc. IEEE Global Telecommun. Conf. (GlobeCom'98)*, Sydney, NSW, Nov. 1998, pp. 1356–1361.

[15] N. Suehiro, N. Kuroyanagi, T. Imoto, and S. Matsufuji, "Very efficient frequency usage system using convolutional spread time signals based on complete complementary code," in *Proc. IEEE Int. Symp. Personal, Indoor and Mobile Radio Commun. (PIMRC2000)*, vol. 2, London, Sep. 2000, pp. 1567–1572.

[16] H.-H. Chen, J.-F. Yeh, and N. Suehiro, "A multicarrier CDMA architecture based on orthogonal complementary codes for new generations of wideband wireless communications," *IEEE Commun. Mag.*, vol. 39, no. 10, pp. 126–135, Oct. 2001.

[17] C. Han, N. Suehiro, J. Chen, N. Kuroyanagi, and M. Nakamura, "Simulation of a parallel transmission system for multipath property to estimate pilot signals and additional chip-shifted information transmission signals," in *Proc. IEEE Int. Workshop Signal Design and Its Applications in Commun. (IWSDA'01)*, Chengdu, China, Sep. 2001, pp. 107–116.

[18] H.-H. Chen, H.-W. Chiu, and M. Guizani, "Orthogonal complementary codes for interference-free CDMA technologies," *IEEE Trans. Wireless Commun.*, vol. 13, no. 1, pp. 68–79, Feb. 2006.

[19] T. Kojima, A. Fujiwara, K. Yano, M. Aono, and N. Suehiro, "Comparison of the two signal design methods in the CDMA systems using complete complementary codes," *IEICE Trans. Found.*, vol. E89-A, no. 9, pp. 2299–2306, Sep. 2006.

[20] P. Z. Fan, N. Suehiro, N. Kuroyanagi, and X. M. Deng, "Class of binary sequences with zero correlation zone," *IEE Electron. Lett.*, vol. 35, no. 10, pp. 777–779, May 1999.

[21] P. Z. Fan and L. Hao, "Generalized orthogonal sequences and their application in synchronous cdma systems," *IEICE Trans. Found.*, vol. E83-A, no. 11, pp. 2054–2069, Nov. 2000.

[22] N. S. Weerasinghe, "Convolutional spreading code-division multiple-access systems with cyclic prefix (CS-CDMA/CP) for downlink transmission," Ph.D. dissertation, Univ. Electro-Communications, Mar. 2007.

[23] N. S. Weerasinghe and T. Hashimoto, "Convolutional spreading CDMA and comparison with the DS-CDMA with RAKE receiver," *IEEE Trans. Commun.*, vol. 54, no. 11, pp. 1918–1922, Nov. 2006.

[24] N. S. Weerasinghe, D. Chen, and T. Hashimoto, "Space-code CS-CDMA systems over MISO frequency-selective rayleigh fading channels," *IEEE Trans. Wireless Commun.*, vol. 7, no. 3, pp. 769–773, Mar. 2008.

[25] S. Zhou, G. B. Giannakis, and C. L. Martret, "Chip-interleaved block-spread code division multiple access," *IEEE Trans. Commun.*, vol. 50, no. 2, pp. 235–248, Feb. 2002.

[26] L. Yue, N. S. Weerashinghe, C. Han, and T. Hashimoto, "Partial multiuser detection for CS-CDMA/CP over multipath channels," *IEEE Trans. Commun.*, vol. 58, no. 8, pp. 2305–2313, Aug. 2010.

[27] N. S. Weerasinghe, C. Han, and T. Hashimoto, "CS-CDMA/CP with ZCZ codes from an M-sequence and its performance for downlink transmission over a multipath fading channel," *IEICE Trans. Found.*, vol. E90-A, no. 6, pp. 1204–1213, Jun. 2007.

[28] D. C. Chu, "Polyphase codes with good periodic correlation properties," *IEEE Trans. Inf. Theory*, vol. 19, no. 4, pp. 531–532, Jul. 1972.

[29] L. Yue, C. Han, N. S. Weerashinghe, and T. Hashimoto, "Performance of coded CS-CDMA/CP with M-ZCZ code over a fast fading channel," *IEICE Trans. Commun.*, vol. E93-B, no. 9, pp. 2381–2388, Sep. 2010.

[30] L. Yue, C. Han, and T. Hashimoto, "CS-CDMA/CP with the chu sequence: A bandwidth-efficient multi-access scheme for fast fading multipath channels," in *Proc. IEEE Int. Conf. Commun. (ICC'11)*, Kyoto, Japan, Jun. 2011, pp. 5–9.

[31] L. Yue, "On the performance of convolutional spreading CDMA with cyclic prefix over fast fading channels," Ph.D. dissertation, Univ. Electro-Communications, Mar. 2011.

[32] C. Han and T. Hashimoto, "Z-connectable complete complementary code and its application in CDMA," in *Proc. IEEE Int. Symp. Infor. Theory (ISIT'09)*, Seoul, Korea, Jun. 2009, pp. 438–442.

[33] C. Han, L. Yue, and T. Hashimoto, "FFT implementable CS-CDMA and its performance under polar clipping noise," in *Proc. IEEE Int. Workshop Signal Design and Its Applications in Commun. (IWSDA'11)*, Chengdu, China, Oct. 2011, pp. 165–168.

[34] H. Mizuyoshi and C. Han, "CS-CDMA system with binary Z-connectable complete complementary codes," in *2019 16th IEEE Annual Consumer Communications Networking Conference (CCNC)*, 2019, pp. 1–2.

[35] M. Tanimoto, H. Sumiyoshi, and M. Komai, "Synchronous spread-spectrum multiplex communication system by using a modified M-sequence," *IEICE Trans. Commun. (in Japanese)*, vol. J67-B, no. 3, pp. 297–304, Mar. 1984.

[36] X. H. Tang, P. Z. Fan, and S. Matsufuji, "Lower bounds on correlation of spreading sequence set with low or zero correlation zone," *IEE Electron. Lett.*, vol. 36, no. 6, pp. 551–552, Mar. 2000.

[37] S.-M. Tseng and M. R. Bell, "Asynchronous multicarrier DS-CDMA using mutually orthogonal complementary sets of sequences," *IEEE Trans. Commun.*, vol. 48, no. 1, pp. 53–59, Jan. 2000.

[38] L. Lu and V. K. Dubey, "Performance of a complete complementary code-based spread-time CDMA system in a fading channel," *IEEE Trans. Veh. Commun.*, vol. 57, no. 1, pp. 250–259, Jan. 2008.

[39] J. W. Craig, "A new, simple and exact result for calculating the probability of error for two-dimensional signal constellations," in *Proc. IEEE Military Commun. Conf. (MILCOM'91)*, vol. 2, McLean, VA, Nov. 1991, pp. 571–575.

[40] M. K. Simon and D. Divsalar, "Some new twists to problems involving the gaussian probability integral," *IEEE Trans. Commun.*, vol. 46, no. 2, pp. 200–210, Feb. 1998.

[41] C. Han, T. Hashimoto, and N. Suehiro, "Constellation-rotated vector OFDM and its performance analysis over Rayleigh fading channels," *IEEE Trans. Commun.*, vol. 58, no. 3, pp. 828–838, Mar. 2010.

[42] G. J. Proakis and S. Masoud, *Digital Communications*, 5th ed. New York: McGraw-Hill, 2008.

[43] E. Balevi and A. O. Yılmaz, "Analysis of frequency domain oversampled MMSE SC-FDE," *IEEE Commun. Lett.*, vol. 20, no. 2, pp. 232–235, Feb. 2016.

[44] W. C. Jakes, *Microwave Mobile Communications*. Piscataway, NJ:IEEE Press, 1994.

[45] Y. Li and X. Huang, "The simulation of independent Rayleigh faders," *IEEE Trans. Commun.*, vol. 50, no. 9, pp. 1503–1514, Sep. 2002.